Chapter 8

# Present-Day Overpressure and Paleopressure Indicators in the Greater Anadarko Basin, Oklahoma, Texas, Kansas, and Colorado

*Click here to return to*
Volume Title Page

By Philip H. Nelson and Nicholas J. Gianoutsos

Chapter 8 of 13
**Petroleum Systems and Assessment of Undiscovered Oil and Gas in the Anadarko Basin Province, Colorado, Kansas, Oklahoma, and Texas—USGS Province 58**
Compiled by Debra K. Higley

U.S. Geological Survey Digital Data Series DDS–69–EE

**U.S. Department of the Interior**
**U.S. Geological Survey**

**U.S. Department of the Interior**
SALLY JEWELL, Secretary

**U.S. Geological Survey**
Suzette M. Kimball, Acting Director

U.S. Geological Survey, Reston, Virginia: 2014



Suggested citation:
Nelson, P.H. and Gianoutsos, N.J., 2014, Present-day overpressure and paleopressure indicators in the greater Anadarko Basin, Oklahoma, Texas, Kansas, and Colorado, chap. 8, *in* Higley, D.K., comp., Petroleum systems and assessment of undiscovered oil and gas in the Anadarko Basin Province, Colorado, Kansas, Oklahoma, and Texas—USGS Province 58: U.S. Geological Survey Digital Data Series DDS–69–EE, 28 p., *http://dx.doi.org/10.3133/ds69EE*.

ISSN 2327-638X (online)

# Contents



## Plates



## Figures

# Appendix 1



# Conversion Factors

Inch/Pound to SI

| Multiply | By | To obtain |
|---|---|---|
| | Length | |
| foot (ft) | 0.3048 | meter (m) |
| mile (mi) | 1.609 | kilometer (km) |
| | Volume | |
| barrel (bbl), (petroleum, 1 barrel=42 gal) | 0.1590 | cubic meter ($m^3$) |
| cubic foot ($ft^3$) | 0.02832 | cubic meter ($m^3$) |
| | Flow rate | |
| cubic foot per day ($ft^3/d$) | 0.02832 | cubic meter per day ($m^3/d$) |
| | Pressure | |
| atmosphere, standard (atm) | 101.3 | kilopascal (kPa) |
| bar | 100 | kilopascal (kPa) |
| pound per square inch ($lb/in^2$) | 6.895 | kilopascal (kPa) |
| | Density | |
| pound per cubic foot ($lb/ft^3$) | 16.02 | kilogram per cubic meter ($kg/m^3$) |
| pound per cubic foot ($lb/ft^3$) | 0.01602 | gram per cubic centimeter ($g/cm^3$) |

Temperature in degrees Celsius (°C) may be converted to degrees Fahrenheit (°F) as follows:
°F=(1.8×°C)+32

Concentrations of chemical constituents in water are given either in milligrams per liter (mg/L) or micrograms per liter (µg/L).

# Present-Day Overpressure and Paleopressure Indicators in the Greater Anadarko Basin, Oklahoma, Texas, Kansas, and Colorado

By Philip H. Nelson and Nicholas J. Gianoutsos

## Abstract

Formation fluids in Pennsylvanian strata of the Anadarko Basin are overpressured throughout the deep part of the basin, as known from previous studies. We take a closer look at the state of overpressuring, documenting the progressive deepening of the top of overpressure from north to south, the increasing vertical extent of overpressure from north to south as strata thicken, the compartmentalization of overpressure in strata of Desmoinesian and Morrowan age, and the areal extent of overpressure in these same strata. Resistivity logs distributed throughout the basin display trendline reversals, with resistivity decreasing with depth rather than continuing to increase along a normal compaction trend. These trendline reversals are interpreted as evidence of an overpressured state in which the pressure can either still be present or else has dissipated, a condition referred to herein as paleopressure. Areas where there are trendline reversals are called paleopressured areas. Paleopressured areas in rocks of Morrowan, Desmoinesian, and Missourian age are more than twice the size of present-day overpressured areas, indicating that the extent of present-day overpressured areas have contracted from paleopressured areas. We suggest that the contraction took place concurrently with the development of normal and subnormal pore pressures on the flanks of the basin when erosional processes exposed Permian and Pennsylvanian strata at the eastern edge of the basin.

## Introduction

This study examines the distribution of present-day overpressure and the evidence that the extent of overpressure at one time occupied an area larger than the present-day distribution of overpressure within the greater Anadarko Basin. Chapter 9 of this report by Nelson and Gianoutsos, which also covers the study area of figure 1, examines the extent and cause of underpressure in the basin. Our two studies on formation fluid pressure were undertaken in support of and in parallel with the work reported by Higley (chapter 7 of this report) and Gaswirth (chapter 5 of this report) on the assessment of oil and gas in the Anadarko Basin. Previous studies dealing with fluid pressure in the basin from Breeze (1970) and Al-Shaieb and others (1994a, b) are cited extensively in this chapter of the report; their study areas are shown in figure 1.

The elevation contours of the Woodford Shale illustrate the structure of the Anadarko Basin (fig. 1); a line drawn through the deepest part of the Woodford Shale serves to locate the deep basin in subsequent figures. Stratigraphic relations of Paleozoic rocks are shown in figure 2; further discussion of the geology of the basin is given by Higley (chapters 5 and 7 of this report). A representative burial history plot (fig. 3) shows that during times of rapid burial, overpressure developed in rocks of the Morrowan, Atokan, Desmoinesian, Missourian, and to a lesser degree in the Virgilian Series, all of Pennsylvanian age, as indicated schematically by the highlighting in figure 3. The areal and stratigraphic distribution of overpressure and its contraction with time is the subject of this chapter of the report.

In this chapter of the report, the term "present-day overpressure" or "overpressure" refers to fluid pressure measurements for which the ratio of measured pressure to the depth of measurement is greater than that of saline formation water, nominally 0.465 pounds per square inch per foot (psi/ft). Moreover, these terms refer to the pressure prior to the production of oil or gas, because pore pressure decreases as hydrocarbons are produced. Measurements of post-production pressures are generally less than pre-production pressure and, although of great interest to reservoir engineers, are considered noise in our studies. The term "paleopressure" refers to overpressure inferred to have existed in the past, either where there is no present-day overpressure or where overpressure in the geologic past was possibly greater than present-day overpressure. In this chapter of the report, paleopressured rock volumes are delineated by the departure of resistivity logs from a normal mudrock compaction trend.

This chapter of the report comprises four parts. In the first part, we review the overpressured zone delineated by Al-Shaieb and others (1994a, b), which is notable because of its large extent and the compartmentalization of pressure within it. Access to the dataset used by Al-Shaieb and others

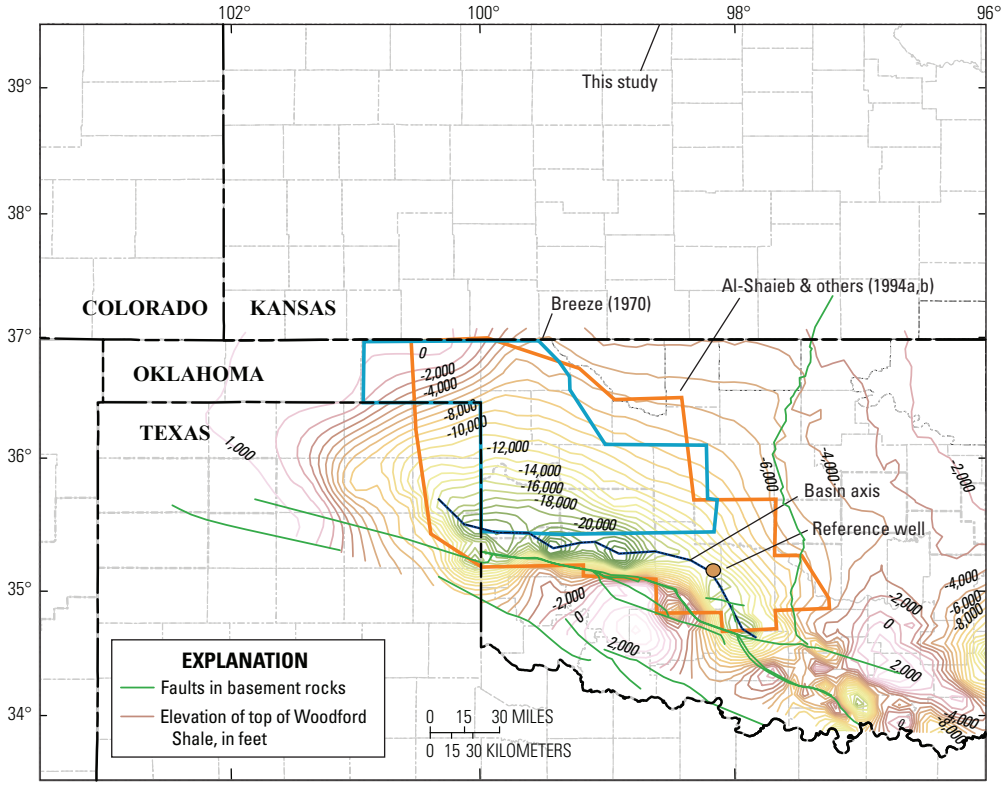


**Figure 1.** Map showing study area encompassing the greater Anadarko Basin in western Oklahoma, the Texas Panhandle, southwestern Kansas, and southeastern Colorado. Areas studied by Breeze (1970) and Al-Shaieb and others (1994a,b) are also shown. Basin axis coincides with deepest structural contours of the Woodford Shale.

(1994a) has made it possible to reformat the pressure-depth plots and produce maps of pressure as a function of geologic age. An important characteristic of the overpressured zone in the Anadarko basin is its preservation for the 250 million years that have elapsed since the presumed onset of overpressure during Permian time. We will return to this point when comparing the overpressured area with the paleopressured area in the third part of this chapter of the report.

In the second part of this chapter of the report, we review previously published work on pressure, salinity, and well log reversals and then, in the third part, describe our own examination of well-log evidence for high pressure in strata of Pennsylvanian and Mississippian age. A decrease of resistivity with increasing depth (rather than an increase along a normal mudrock compaction trend) is an indicator that rocks are not normally compacted (Bigelow, 1994). The lack of complete compaction can be attributed to either of two causes. (1) During burial, the rocks were partially prevented from compacting by pore pressure that remained higher than normal. This can happen if pore water is prevented from escaping from the pore space, so the pore water bears part of the vertical stress, a phenomenon referred to as disequilibrium compaction. (2) Excess pressure arises during the generation of oil and gas because of a volume increase in the amount of fluid in the pore space, causing microcracks to open within the rock. Microcracks that opened during generation of excess pressure remain partially open, with consequent reductions of resistivity and sonic velocity. Regardless of how the excess pressure was generated, if that pressure is maintained, either in whole or in part into the present day, then the excess pressure is measurable as overpressure. If the pressure from either of these two causes was not maintained but diminished either partly or entirely at some time in the past, then we refer to it as paleopressure. In this chapter of the report, the reversals in resistivity logs are called a "paleopressure indicator" and the rock volume thus affected is referred to as being paleopressured.

In the fourth part of this chapter of the report, we compare the overpressured and paleopressured areas with levels of thermal maturity obtained from basin modeling, finding that the highest levels of thermal maturity nearly coincide with the highest levels of present-day overpressure. We show that the area of the Anadarko Basin where resistivity reversals are present (the geographic extent of paleopressure) is greater than (and includes) the present-day overpressured zone delineated by Al-Shaieb and others (1994a, b). The main finding of this chapter of the report is the inferred contraction in horizontal

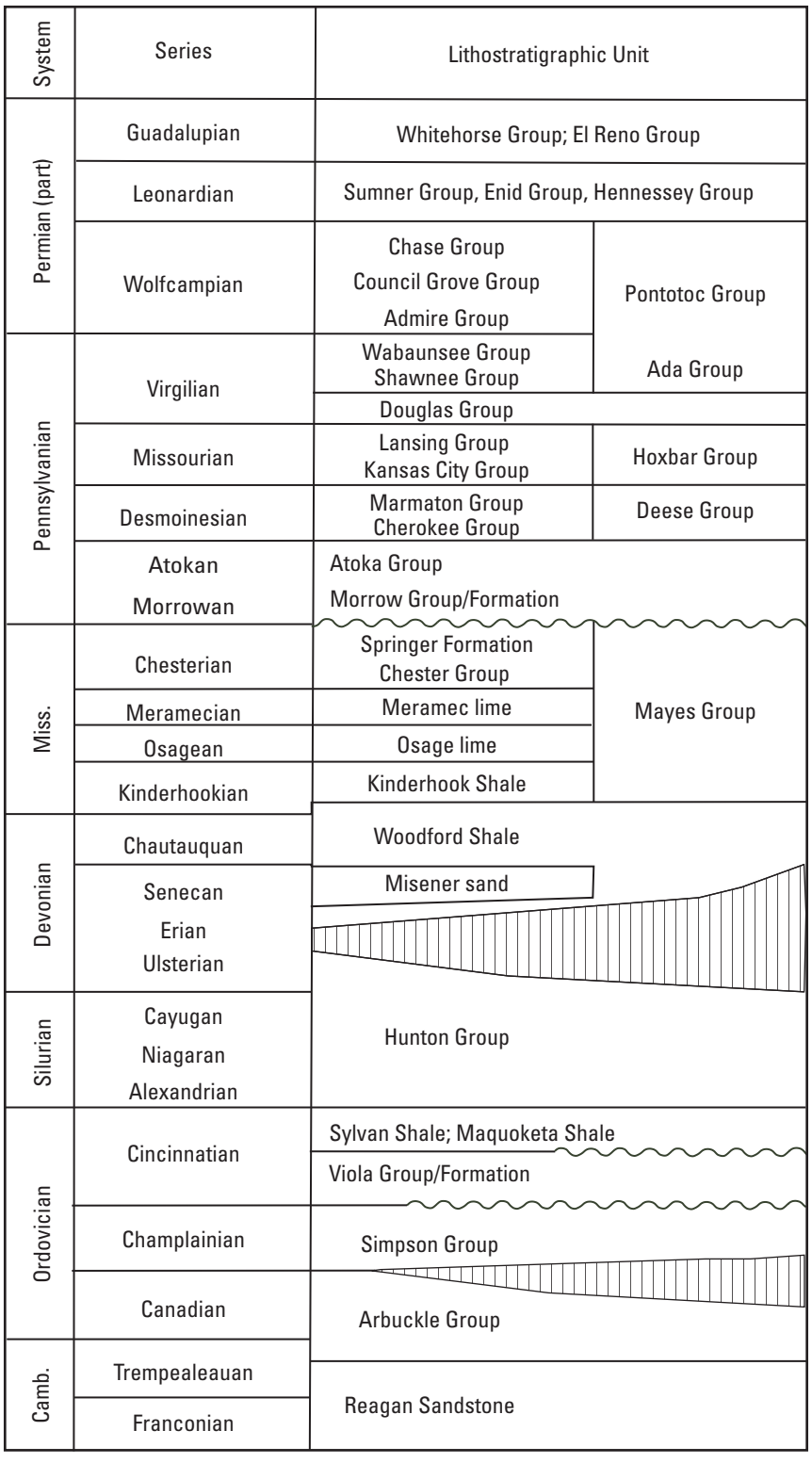


**Figure 2.** Stratigraphic chart for the Anadarko Basin, from Higley (chapter 3 of this report). Wavy lines represent unconformities. Areas with vertical lines represent periods of non-deposition. (Camb., Cambrian; Miss., Mississippian).

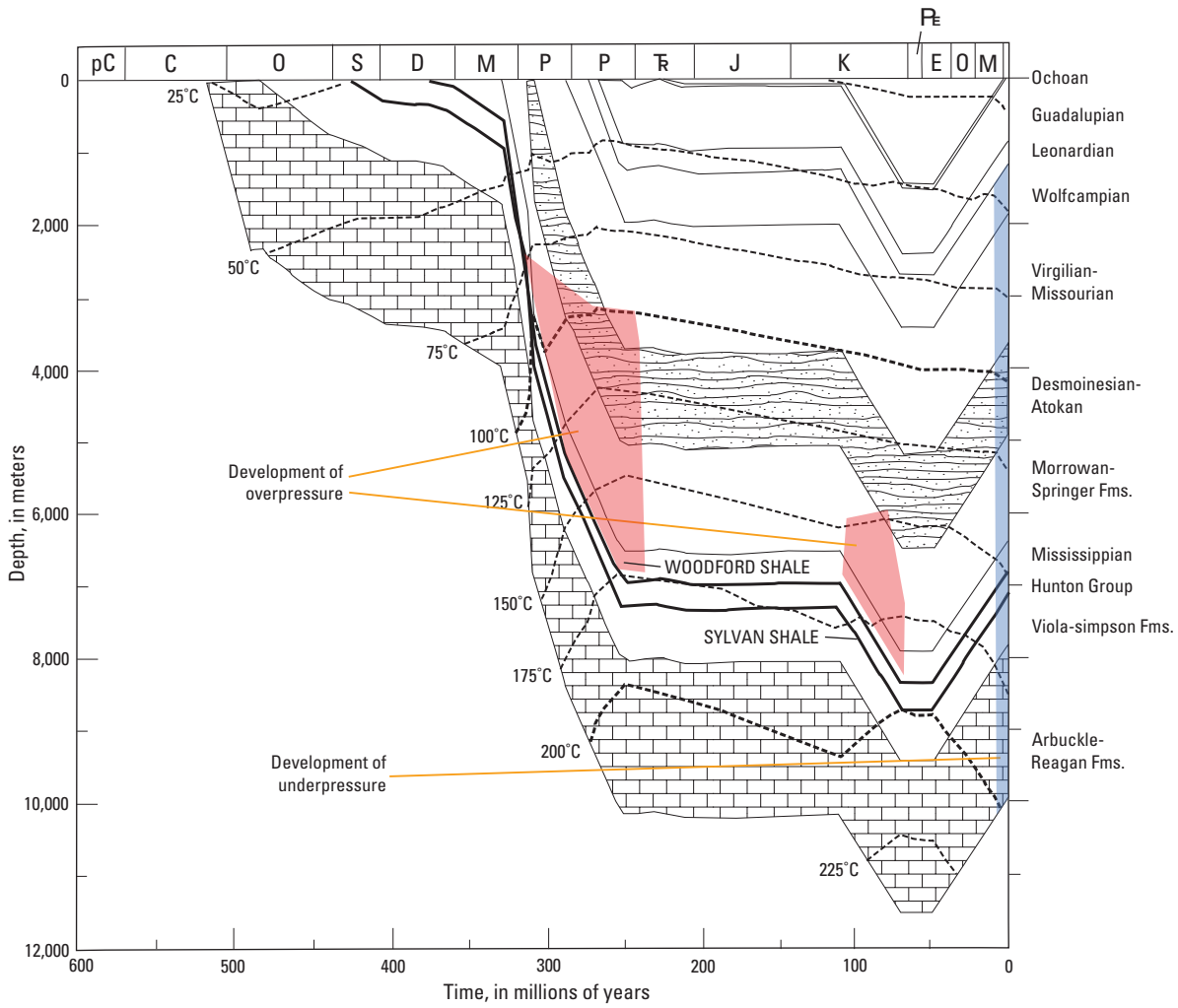


**Figure 3.** Burial history for the Ferris 1-28 well, from Carter and others (1998). Well location is shown in figure 1. The times when overpressure and underpressure probably developed are highlighted. (pC, Precambrian; C, Cambrian; O, Ordovician; S, Silurian; D, Devonian; M, Mississippian; IP, Pennsylvanian; P, Permian; Tr, Triassic; J, Jurassic; K, Cretaceous; Pe, Paleocene; E, Eocene; O, Oligocene; M, Miocene; FMS., Formations).

and vertical extent of the paleopressured rock volume to its smaller present-day overpressured volume. Some speculative ideas on the timing of the contraction are included in the fourth part of the chapter.

## Overpressure in Rocks of Pennsylvanian and Mississippian Age

Al-Shaieb and others (1994a, b) used 4,439 reservoir-pressure data points to map the pressure regime in the Oklahoma and Texas portions of the Anadarko Basin. Sources were (1) pressures calculated from static initial wellhead shut-in pressures (2,579 points), (2) shut-in pressures from drillstem tests (1,787 points), and (3) recorded bottom-hole pressures from P/Z plots in production records (73 points). Their primary finding was the delineation of a large overpressured volume called the megacompartment complex (designated Level 1, with lateral dimensions of 100 miles) that contains sub-compartments within a single stratigraphic interval (Level 2 compartments, with lateral dimensions of tens of miles). Nested within Level 2 compartments are Level 3 compartments, with lateral dimensions of a few miles, that are linked to depositional facies within reservoirs. The megacompartment complex is bounded by the Woodford Shale at the base, and by major structural offsets on the south. The top of the overpressured zone lies between depths of 7,500 and 10,000 feet (ft) and crosses stratigraphic boundaries. The northern edge is formed by the convergence of the top and basal boundaries as strata thin to the north.

We have combined data from Al-Shaieb and others (1994a) with data extracted from a commercial database (IHS Energy, 2009) to provide illustrative examples of pressure-depth plots from various parts of the basin (fig. 4). These examples demonstrate underpressure in the northwestern part of the basin (*A* and *B* of fig. 4), normal pressure on the northern flank (*C* of fig. 4), and overpressure in the deep basin (*D* and *E* of fig. 4). Underpressure is revealed by the slight gap between the mud-weight pressures, which track the 0.465 psi/ft line, and the drillstem-test pressures in *A* and *B* of figure 4. Underpressure in the Missourian-Virgilian and Morrowan rocks was mapped but not discussed by Al-Shaieb and others (1994a). The characterization and cause of underpressure in the greater Anadarko Basin is the subject of chapter 9 of this report by Nelson and Gianoutsos. Normal pressure is shown where the drillstem-test pressures coincide with the mud-weight pressures on the 0.465 psi/ft line as illustrated in figure 4*C* and at depths shallower than 10,000 ft in figure 4*D*. (Because many of the pressures from drillstem tests are lower than the actual pore pressure, because of either inadequate tests or to reservoir depletion, only the righthand edge of the drillstem-test data field should be considered as representative of pore pressure.)

Overpressure is present in rocks of Desmoinesian and Morrowan age as shown in figure 4*D*. Evidence of the compartmentalization cited by Al-Shaieb and others (1994a) is seen where the pressures in Morrowan rocks reach a maximum pressure-depth ratio of nearly 1.0 psi/ft, whereas the pressures in Desmoinesian rocks reach a lesser maximum of nearly 0.9 psi/ft. As pore pressure builds, drillers increase the mud weight to maintain control of the well while drilling. The mud-weight and drillstem-test pressures shown in *D* and *E* of figure 4 are consistent with the pressures compiled by Al-Shaieb and others (1994a), keeping in mind that the two datasets were not taken from the same wells but represent all wells with data in a 30- by 30-mile area.

The complete dataset for Oklahoma of Al-Shaieb and others (1994a) is displayed in 28 pressure-depth plots in plate 1. Each pressure-depth plot incorporates all data in a block of 8 to 15 townships. Many of the blocks (blocks B, C, F–O, R, and S on the index map in plate 1) are three townships (18 miles) in the south-north direction and four townships (24 miles) in the west-east direction; other blocks have comparable areas but different shapes. Grouping the data in this way permits inspection of the pressure-depth profiles and selection of the top of overpressure as a function of location; the pressure-depth trends cannot be examined in individual wells because a single well typically contributes only a few pressure measurements. Some observations regarding the relations among pressure, depth, and location within the basin are:

(1) The presence of megacompartments pointed out by Al-Shaieb and others (1994a, b) can be seen as a step increase in pressure with depth in Desmoinesian and Morrowan age rocks in blocks H, I, L, and M. Another step increase in pressure with depth takes place between Atokan/Desmoinesian and Morrowan rocks in block S.

(2) Below the overpressured intervals in Desmoinesian and Morrowan rocks in blocks H, I, J, and L, pressures return to normal in underlying rocks of Silurian age. The pressure regression supports the statement of Al-Shaieb and others (1994a, b) that the Devonian Woodford Shale is the base of the overpressured interval. In other blocks, the return to normal pressure at depth cannot be observed because rocks deeper than Morrowan were not penetrated. An exception occurs in the southeastern part of the study area in blocks Z and ZZ where Ordovician rocks are overpressured.

(3) Overpressured conditions prevail to a depth of 20,000 ft in rocks of Mississippian age in blocks X and Y.

(4) Normal to subnormal pressures prevail in blocks A–E on the northern flank of the area. The northernmost appearance of overpressure in Desmoinesian and Morrowan rocks is in blocks F and G in portions of T. 18-20 N. Normal pressures prevail in rocks of various ages on the east side of the basin in blocks Q, W, and YY.

(5) In general, the top of overpressure deepens from north to south. The top of overpressure is here defined as the depth below which several points have pressure-depth ratios exceeding 0.5 psi/ft. Examining the north to south progression in R. 11-14 W., the top of overpressure is located at depths of approximately 6,500 ft in block G, 8,100 ft in block K, 10,100 ft in block O, and 13,000 ft in block U. A similar deepening of the top of overpressure can be observed in blocks F, J, N, and T in R. 15-18 W.

The top of overpressure was determined for each of the 28 blocks shown in the index map on plate 1. Because the top of overpressure is determined by the depth of the shallowest overpressured measurements, and because there may be overpressured rocks above that depth for which no pressure was determined, it is likely that the top of overpressure is shallower in those blocks with sparse data, but it is unlikely that the top of overpressure is deeper than the selected depth. The depth of the top of overpressure and the average surface elevation was determined for each of the 28 blocks, and the elevation of the top of overpressure relative to sea level was then computed. The resulting contour map (fig. 5), based on 28 points and with a limited extension into the Texas Panhandle, shows the basinward drop in the top of overpressure from elevations above -6,000 ft to elevations deeper -10,000 ft. No comparable map was presented by Al-Shaieb and others (1994a), although the map in figure 5 appears compatible with the top of overpressure illustrated on a cross section (Al-Shaieb and others 1994a, figure 11).

Al-Shaieb and others (1994a) presented pressure-contour maps of the (1) Missourian/Virgilian interval (showing mostly normal pressures), (2) Desmoinesian Red Fork Sandstone (showing pressure-depth ratios exceeding 0.8 psi/ft), (3) Morrowan Series (showing pressure-depth ratios exceeding 0.9 psi/ft), and (4) Hunton Group (showing a return to normal pressure below the base of the Woodford Shale, with the exception of one overpressured value of 0.74 psi/ft attributed to an isolated Hunton compartment). Using their digital dataset augmented by pressure data from IHS Energy (2009), we

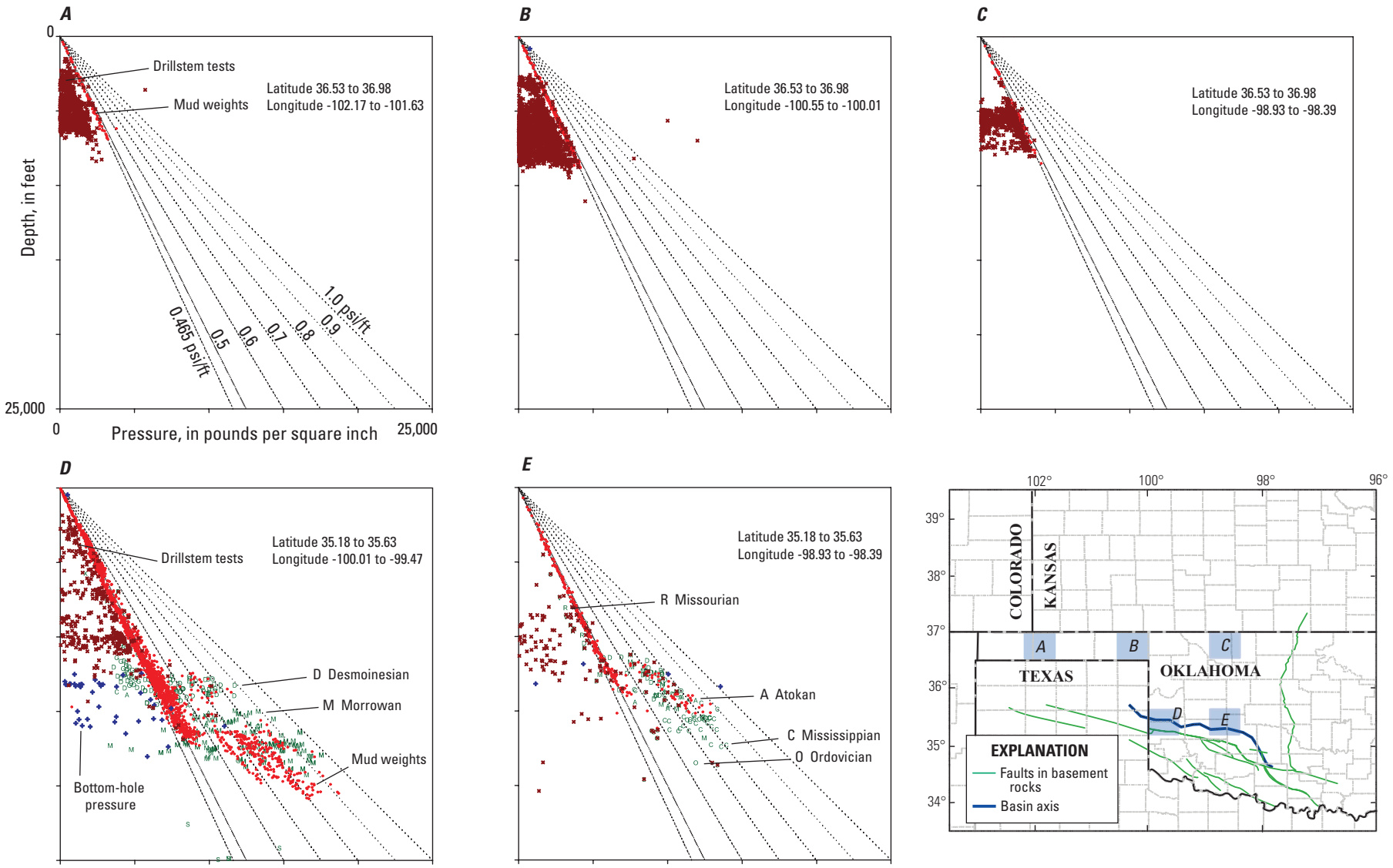


**Figure 4.** Plots of pressure against depth for five areas *A* through *E* in the greater Anadarko Basin. Each plot contains pressure data from wells within a 30- by 30-mile area located in the index map. Faults in basement rocks bound the eastern and southern parts of the basin. Pressure data designated by green letters representing geologic periods are from Al-Shaieb and others (1994a). Pressure data from drillstem tests, bottom-hole pressures, and mud weights are taken from IHS Energy (2009).

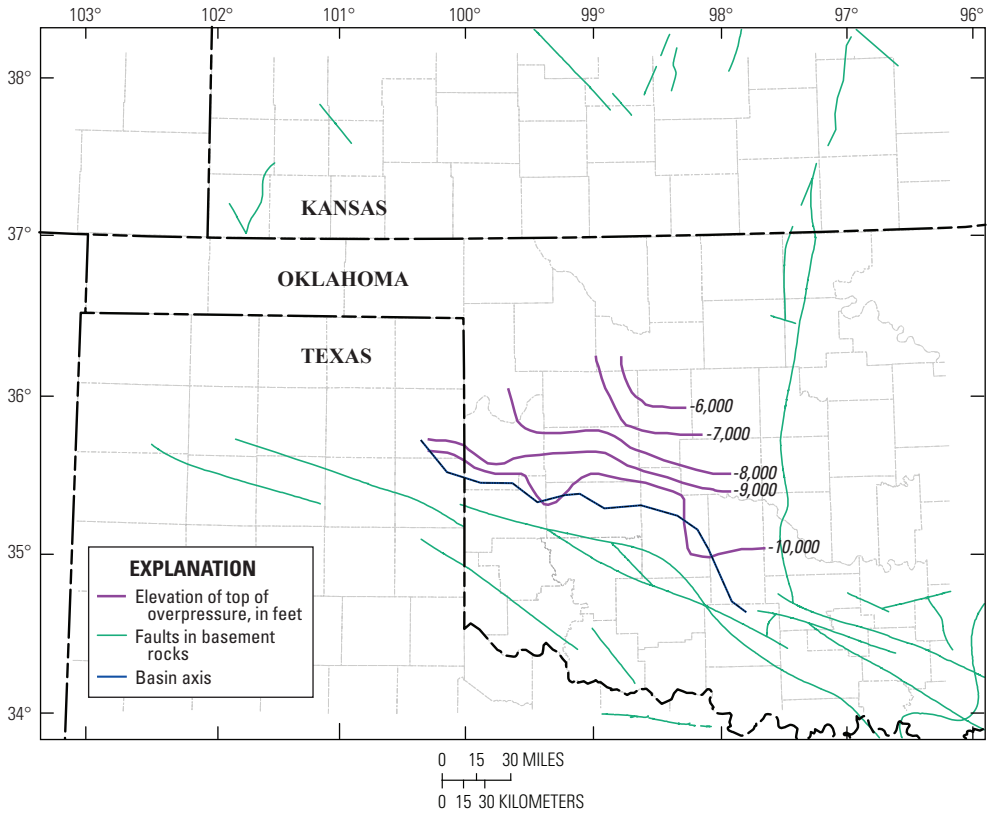


**Figure 5.** Map showing elevation of top of overpressure, based on data displayed in plate 1.

created outlines of present-day overpressure for the Morrowan and Desmoinesian series (figs. 6 and 7). The Desmoinesian outline (fig. 6), which includes pressures measured in rocks of Desmoinesian age, extends farther north and west than the area mapped by Al-Shaieb and others (1994a), which is restricted to pressures measured in the Desmoinesian Red Fork Sandstone. The outer boundary includes measurements with pressure-depth ratios greater than 0.5 psi/ft and the inner boundary shows the area of highest pressure with pressure-depth ratios greater than 0.7 psi/ft. The southern edge of the outer boundary is drawn in close proximity to the bounding fault.

The Morrowan outline (fig. 7), which includes pressures measured in rocks of Morrowan and Springer age, follows the outline established by Al-Shaieb and others (1994a) except in Dewey County of Oklahoma, where the outline extends roughly 10 miles farther to the north. The eastern edge coincides with the truncation edge of Morrowan age rocks. The southern edge is drawn in close proximity to the bounding fault. Pressure compartments within the Morrow and Springer Formations (fig. 8*A*) were outlined by Powley (1984) in a study for Amoco. Amoco data were incorporated in the work of Al-Shaieb and others (1994a), and the boundaries of the two studies are similar. Moreover, Powley (1984) delineated nine pressure compartments within the Morrow and Springer Formations, each characterized by distinctive pressure-elevation relations with a unique potentiometric surface $H$ calculated from $H(\text{ft}) = Z(\text{ft}) + P(\text{psi})/0.465$, where $Z$ is elevation and $P$ is pressure. Eight of the nine compartments are overpressured, as shown by values of $H$ that are greater than normal values of 2,000 to 3,500 ft (fig. 8*A*). Pressure-elevation plots for three of the nine areas demonstrate that differences in pressure between compartments is on the order of several thousand psi and that pressure gradients are around 0.465 psi/ft (fig. 8*B*). The determination of pressure-depth gradients of 0.465 psi/ft, equivalent to the density of a moderately saline brine, shows that elevated hydrostatic gradients prevail over substantial areas within strata of Morrowan and Springer age. Thus, these overpressured compartments are water-dominated, and gas and oil accumulations within the compartments can be expected to be in buoyant equilibrium with water.

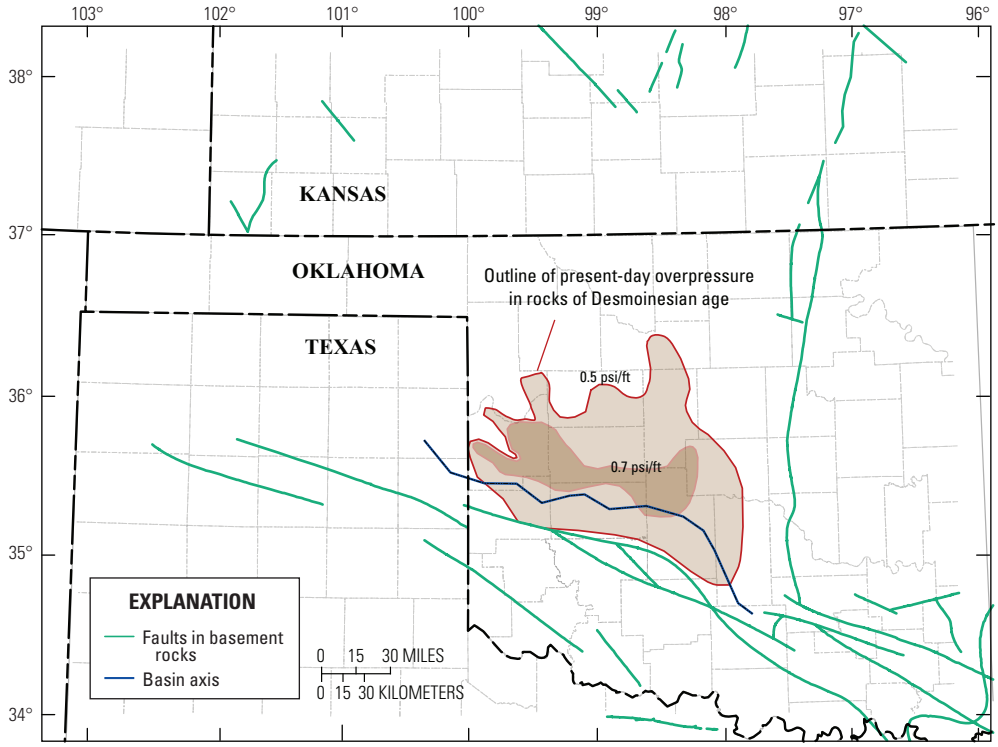


**Figure 6.** Map showing outline of present-day overpressure in rocks of Desmoinesian age, based on data from Al-Shaieb and others (1994a) and augmented with pressure data from IHS Energy (2009). Contour lines and shading represent the ratio of pressure to depth in pounds per square inch per foot (psi/ft).

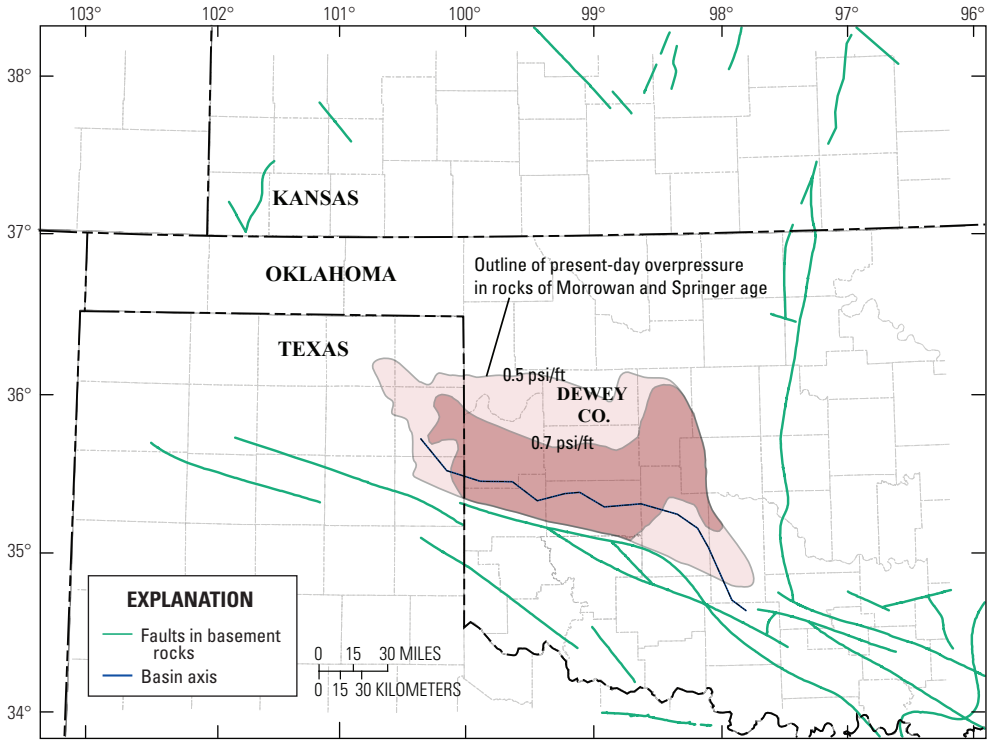


**Figure 7.** Map showing outline of present-day overpressure in rocks of Morrowan and Springer age, based on data from Al-Shaieb and others (1994a) and augmented by pressure data from IHS Energy (2009). Contour lines and shading represent the ratio of pressure to depth in pounds per square inch per foot (psi/ft).

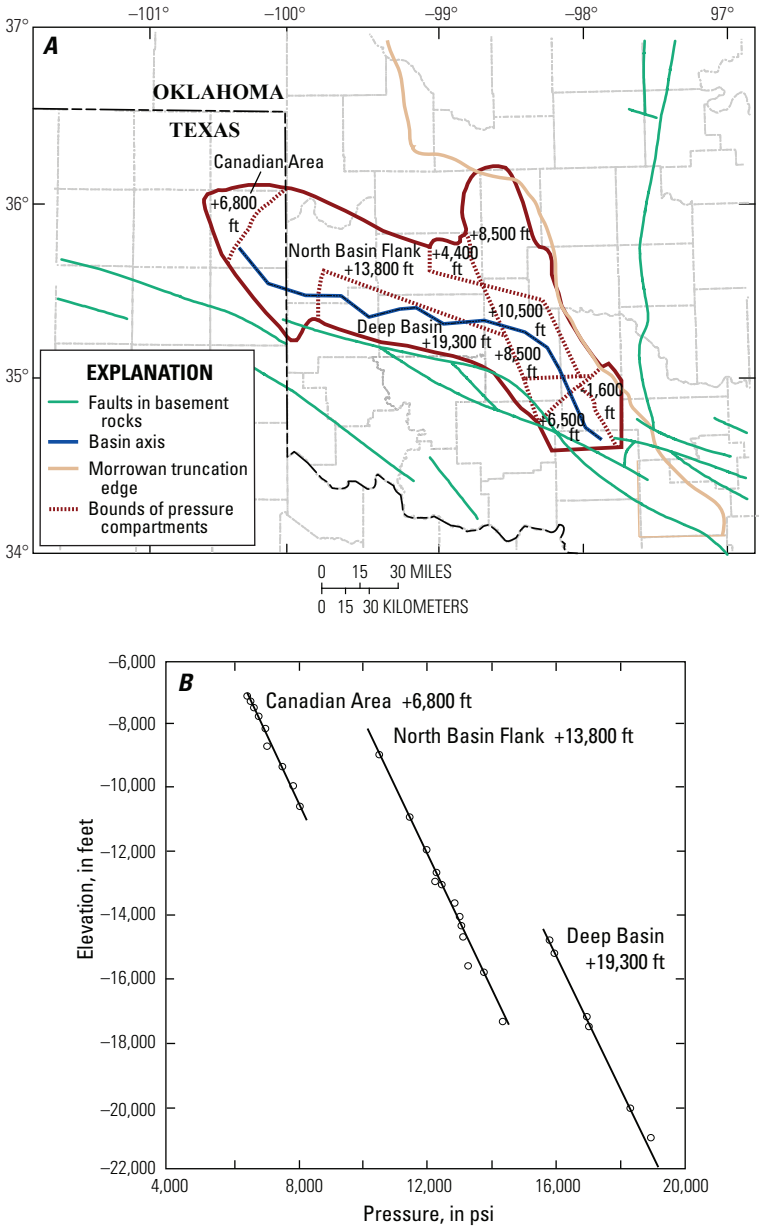


**Figure 8.** *A*, Nine overpressured compartments in Morrowan and Springer age rocks, from Powley (1984). Elevation in feet (ft) of potentiometric surface H is given for each area. *B*, Pressure as a function of elevation for three overpressured areas in Morrow and Springer Formations, from Powley (1984). Pressure data are from oil and gas fields and individual wells. Each line has a slope of 0.465 pounds per square inch per foot (psi/ft).

## Indicators of Paleopressure from Previous Work

In the course of investigating the cause of underpressure in the Morrowan sandstones of the northwestern Anadarko Basin, Breeze (1970) examined the characteristics of sonic logs, resistivity logs, and formation water salinity in six wells (fig. 9). The data from Breeze (1970), presented in the first three columns of figures 10*A*–10*F* of this chapter of the report, show increasing resistivity and decreasing sonic slowness[1] of mudrocks in the upper part of each well, followed by reversals in these trends in the lower part of each well. The maximum resistivity at the top of the reversal in the six wells is about 10 ohm-m, and the minimum sonic slowness is 70 to 75 (µs/ft). However, the density logs show a steady increase of density with depth with no reversals and hence do not show evidence of undercompaction (density logs shown by Breeze for the six wells of figures 10*A*–10*F* are not reproduced here).

[1] Sonic slowness, also called sonic travel time, is the inverse of sonic velocity. Slowness is measured by sonic logs and presented in units of microseconds per foot (µs/ft). The term "slowness" will be used throughout the remainder of this chapter of the report.

Pressure data, shown in the right-hand plot of figures 10*A*-10*F*, behaves quite differently than the sonic and resistivity logs and formation water salinities. Present-day pressure varies from greater than hydrostatic (overpressured) in the Neely 1 well (fig. 10*A*), which is the southeasternmost of the six wells, to moderately overpressured in the Cheyenne-Arapahoe Unit 1 well (fig. 10*B*), to normally pressured in the Raymond Moss and Knabe 1 wells (figs. 10*C* and 10*D*), to underpressured in the Kamp and Fox wells (figs. 10*E* and 10*F*). Thus, the present-day pressure ranges from overpressure to underpressure in a line of wells (fig. 9) in which the sonic and resistivity logs suggest overpressured conditions in mudrocks. Breeze (1970, p. 73) decided that the conditions producing the well log reversals differed from present-day conditions, "It is therefore concluded that the entire area was once subject to a similar history of deposition that left undercompacted shales as evidence." The thesis of this report follows the same line of reasoning.

The salinity of formation water, which is around 100,000 ppm total dissolved solids in the upper part of each well, decreases in the lower part of each well to values about one-third of the values in the upper part (figs. 10*A*–10*F*). Water chemistry over a more extensive area was also reported by

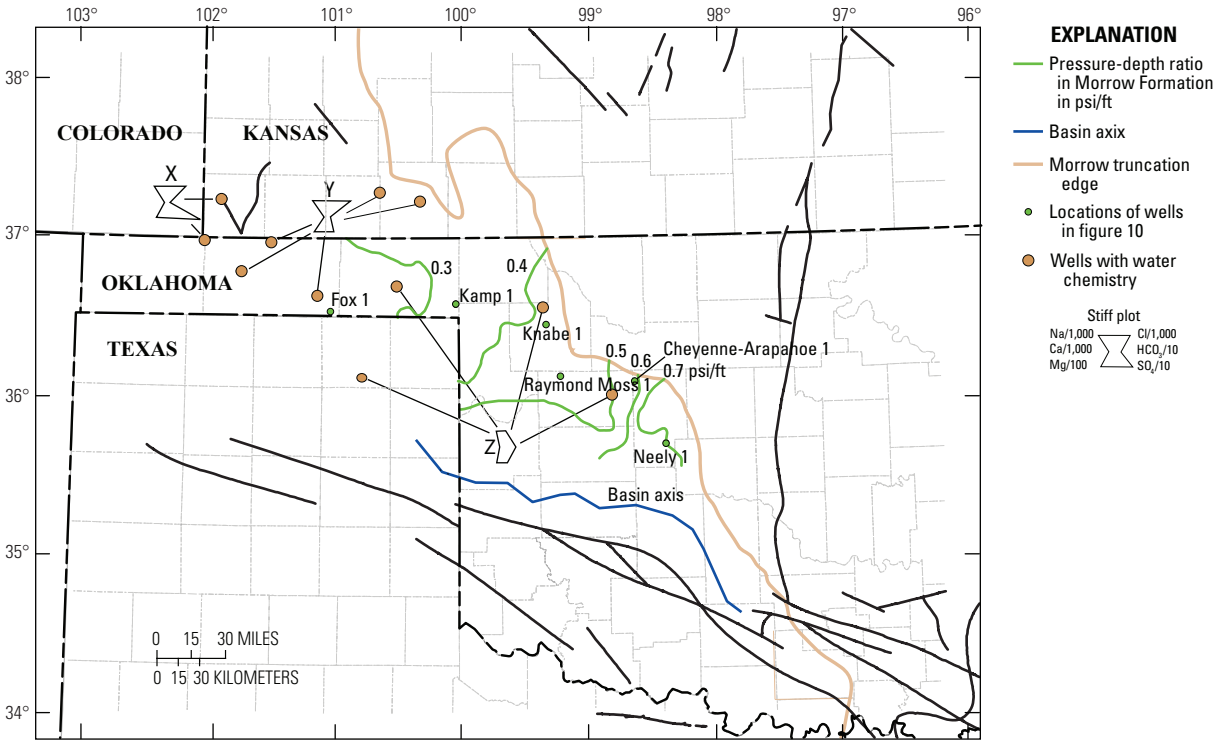


**Figure 9.** Map showing contours of present-day pressure-depth ratios in the Morrow Formation, showing change from overpressure [greater than 0.5 pounds per square inch per ft (psi/ft)] to underpressure (less than 0.4 psi/ft), based on data from Breeze (1970). Six named wells (small green circles) show well-log indicators of paleopressure, as interpreted by Breeze (1970). Water chemistry falls into three distinct types as shown by Stiff plots labeled X, Y, and Z, from Dickey and Soto (1974). Each brown circle is the locus of several wells from which water samples were taken.

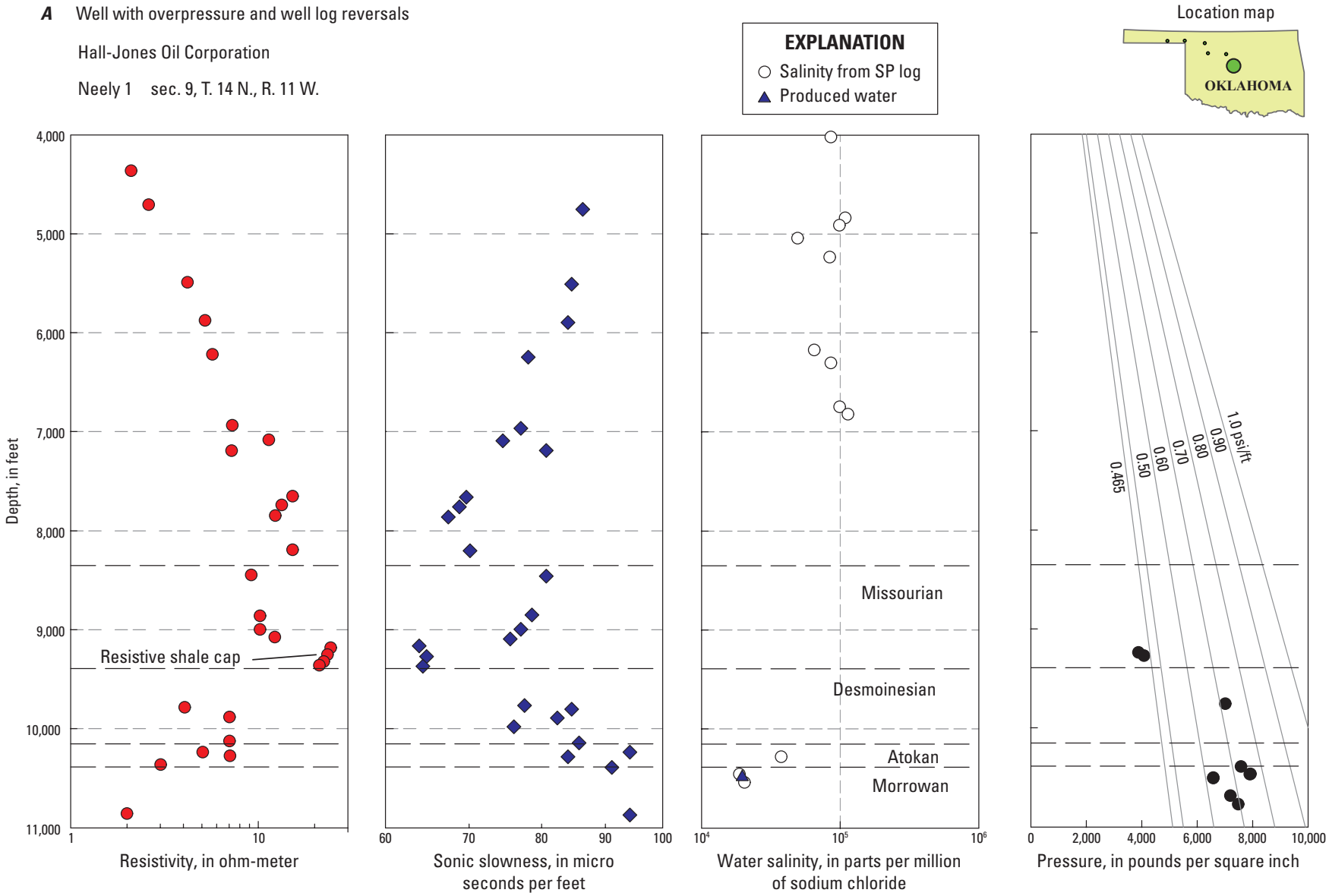


**Figure 10.** Graphs showing indicators of paleopressure in mudrocks from resistivity, sonic, and self potential (SP) logs in six wells from Breeze (1970). Well locations are shown in figure 9 and in the inset map. Salinity of produced water from a nearby well is also from Breeze (1970). Pressure data from wells within a 3- to 10-mile distance from the designated well taken from Al-Shaieb and others (1994a). *A*, Neely 1 well; *B*, Cheyenne-Arapahoe Unit 1 well; *C*, Raymond Moss 1 well; *D*, Knabe 1 well; *E*, Kamp 1 well; and *F*, Fox 1 well.

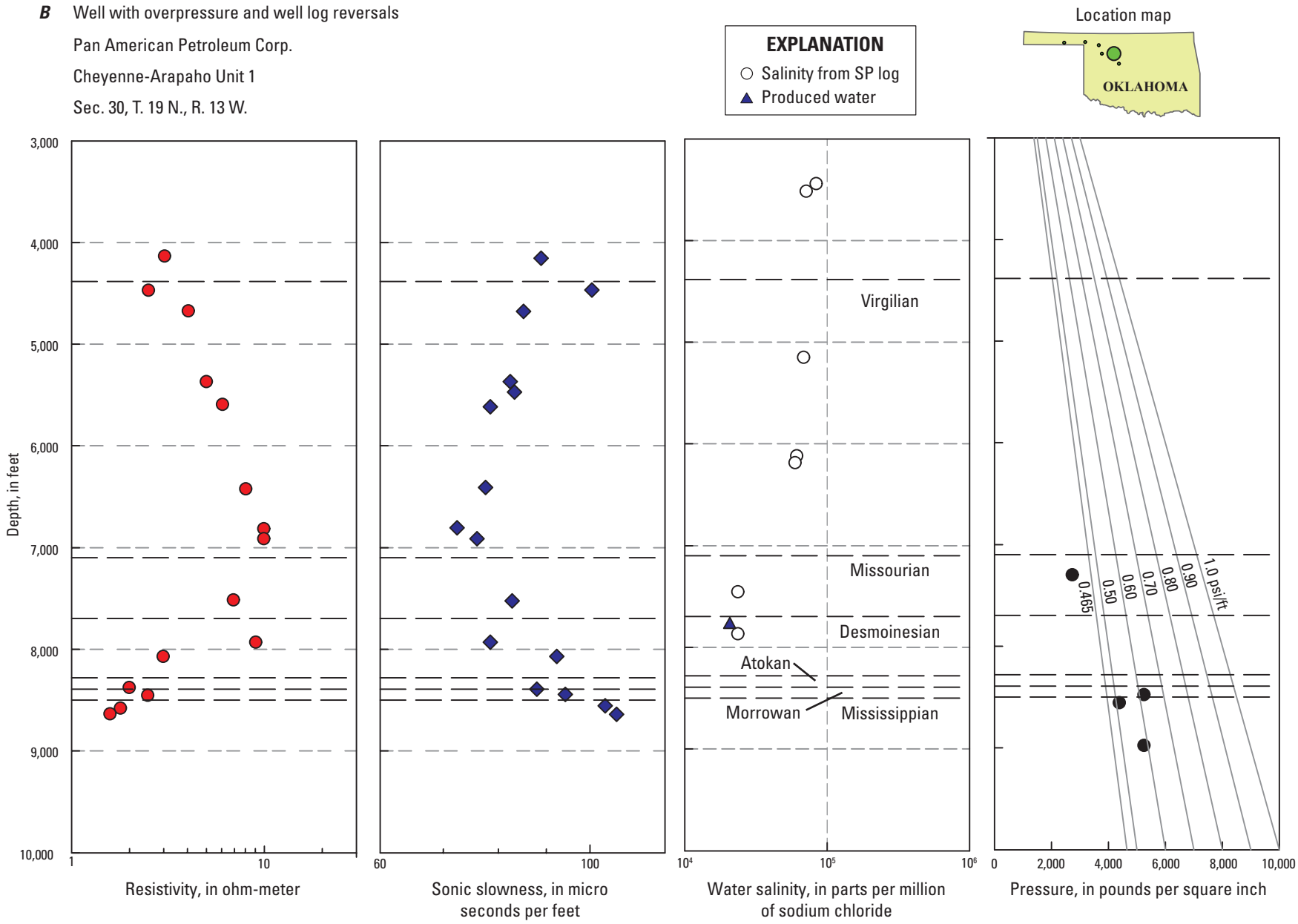


**Figure 10.** Graphs showing indicators of paleopressure in mudrocks from resistivity, sonic, and self potential (SP) logs in six wells from Breeze (1970). Well locations are shown in figure 9 and in the inset map. Salinity of produced water from a nearby well is also from Breeze (1970). Pressure data from wells within a 3- to 10-mile distance from the designated well taken from Al-Shaieb and others (1994a). *A*, Neely 1 well; *B*, Cheyenne-Arapahoe Unit 1 well; *C*, Raymond Moss 1 well; *D*, Knabe 1 well; *E*, Kamp 1 well; and *F*, Fox 1 well.—Continued

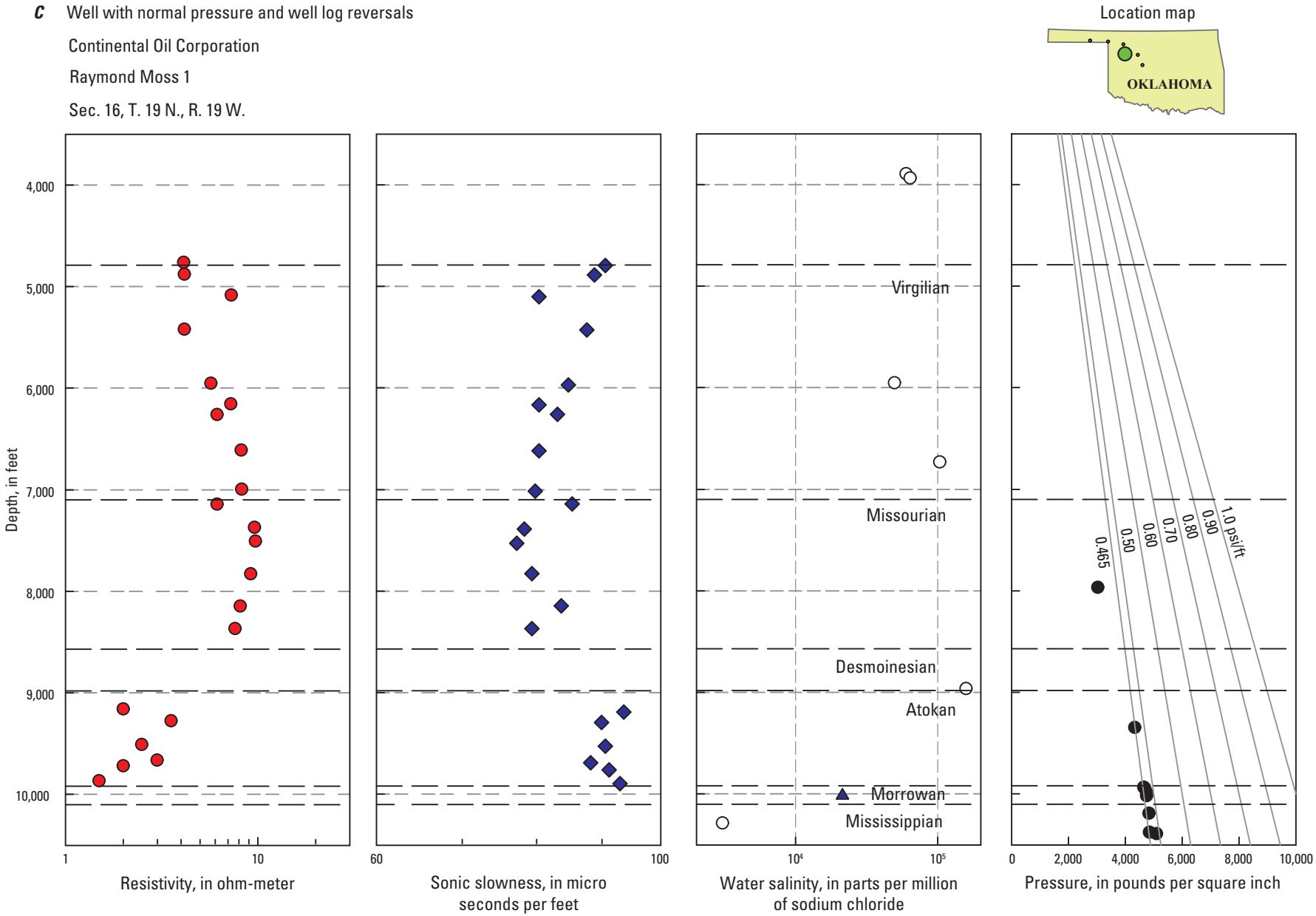


**Figure 10.** Graphs showing indicators of paleopressure in mudrocks from resistivity, sonic, and self potential (SP) logs in six wells from Breeze (1970). Well locations are shown in figure 9 and in the inset map. Salinity of produced water from a nearby well is also from Breeze (1970). Pressure data from wells within a 3- to 10-mile distance from the designated well taken from Al-Shaieb and others (1994a). *A*, Neely 1 well; *B*, Cheyenne-Arapahoe Unit 1 well; *C*, Raymond Moss 1 well; *D*, Knabe 1 well; *E*, Kamp 1 well; and *F*, Fox 1 well.—Continued

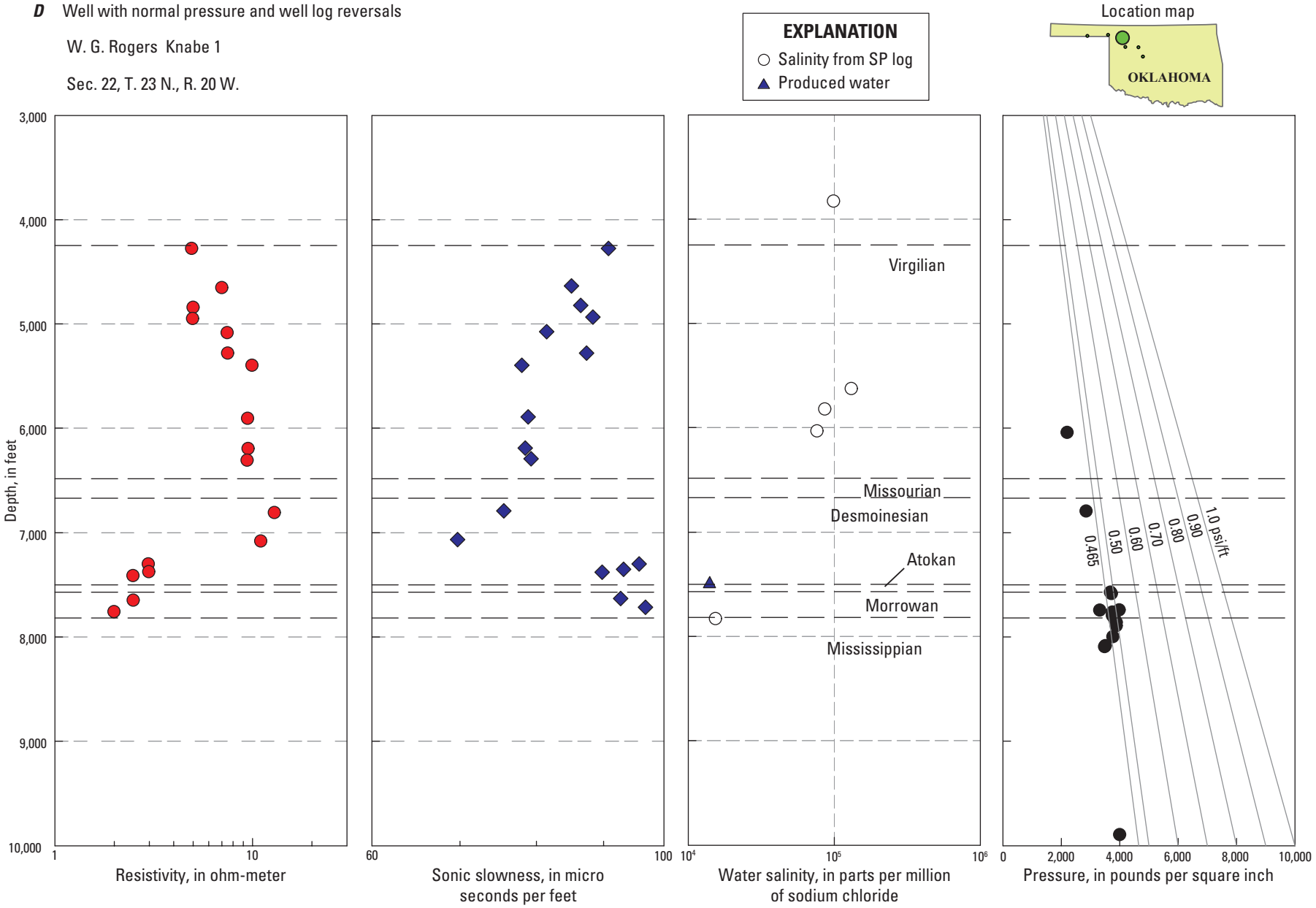


**Figure 10.** Graphs showing indicators of paleopressure in mudrocks from resistivity, sonic, and self potential (SP) logs in six wells from Breeze (1970). Well locations are shown in figure 9 and in the inset map. Salinity of produced water from a nearby well is also from Breeze (1970). Pressure data from wells within a 3- to 10-mile distance from the designated well taken from Al-Shaieb and others (1994a). *A*, Neely 1 well; *B*, Cheyenne-Arapahoe Unit 1 well; *C*, Raymond Moss 1 well; *D*, Knabe 1 well; *E*, Kamp 1 well; and *F*, Fox 1 well.—Continued

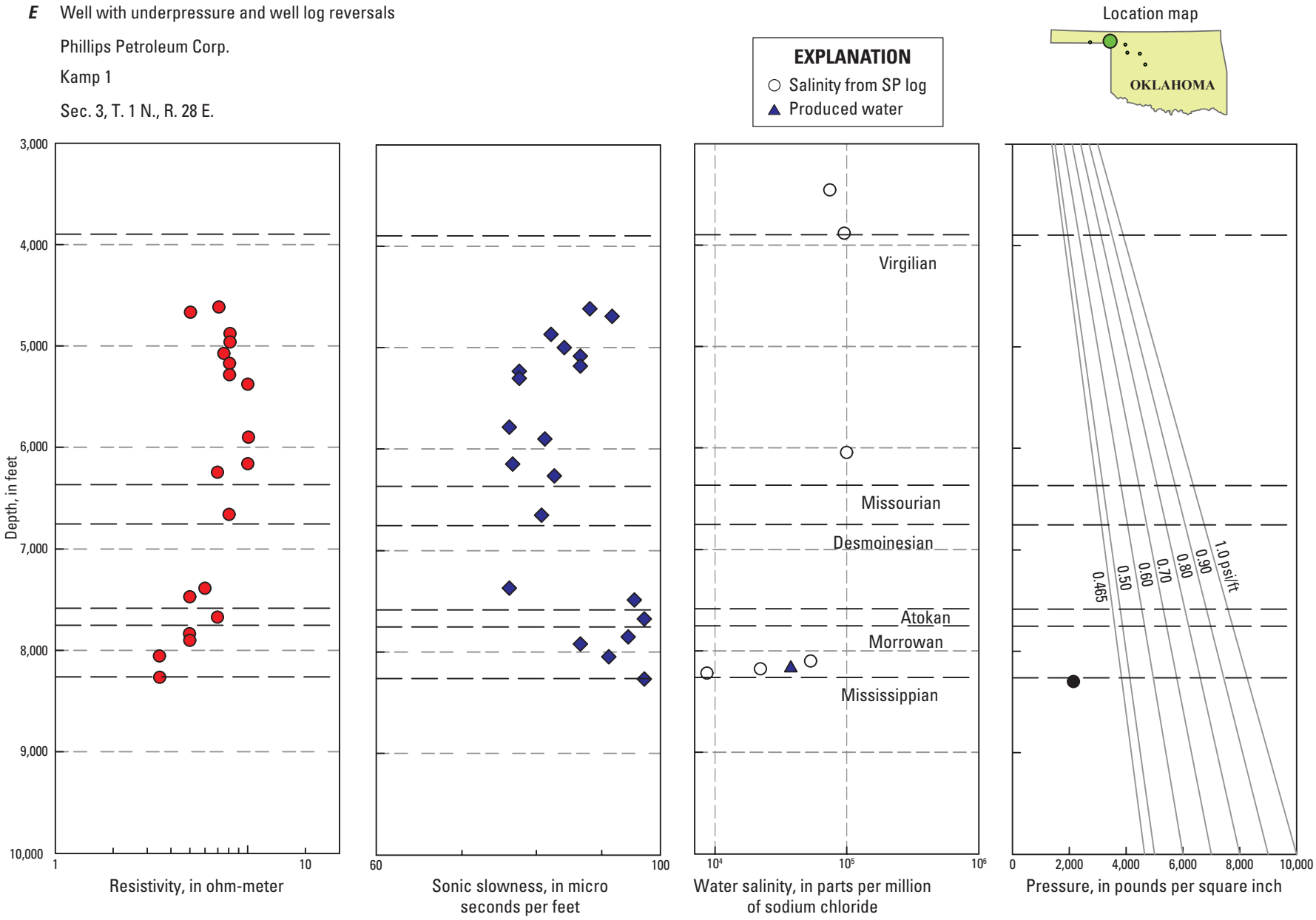


**Figure 10.** Graphs showing indicators of paleopressure in mudrocks from resistivity, sonic, and self potential (SP) logs in six wells from Breeze (1970). Well locations are shown in figure 9 and in the inset map. Salinity of produced water from a nearby well is also from Breeze (1970). Pressure data from wells within a 3- to 10-mile distance from the designated well taken from Al-Shaieb and others (1994a). *A*, Neely 1 well; *B*, Cheyenne-Arapahoe Unit 1 well; *C*, Raymond Moss 1 well; *D*, Knabe 1 well; *E*, Kamp 1 well; and *F*, Fox 1 well.—Continued

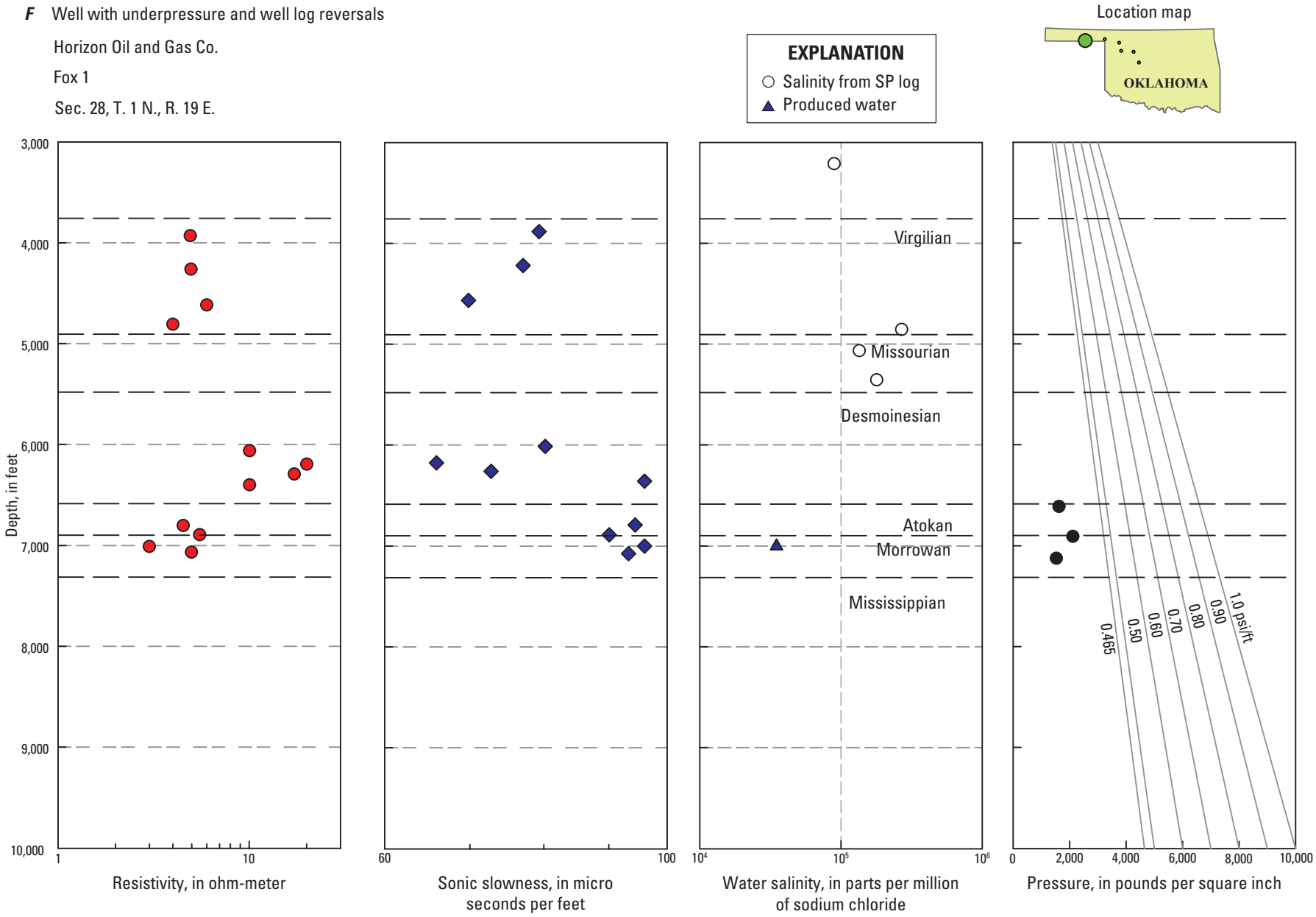


**Figure 10.** Graphs showing indicators of paleopressure in mudrocks from resistivity, sonic, and self potential (SP) logs in six wells from Breeze (1970). Well locations are shown in figure 9 and in the inset map. Salinity of produced water from a nearby well is also from Breeze (1970). Pressure data from wells within a 3- to 10-mile distance from the designated well taken from Al-Shaieb and others (1994a). *A*, Neely 1 well; *B*, Cheyenne-Arapahoe Unit 1 well; *C*, Raymond Moss 1 well; *D*, Knabe 1 well; *E*, Kamp 1 well; and *F*, Fox 1 well.—Continued

Dickey and Soto (1974), as shown by the Stiff diagrams in figure 9. Water types X, Y, and Z of figure 9 were defined by Dickey and Soto (1974) to distinguish three compositional groups. Water chemistry changes from moderate salinity (30,000–80,000 mg/L) sulfate waters of the chloride-calcium type X in the northwest, to typical connate high-salinity (100,000–200,000 mg/L) brines of the chloride-calcium type Y, to a low-salinity (10,000–30,000 mg/L) high-bicarbonate type Z. The type Z samples are located in the area studied by Breeze. Dickey and Soto (1974, p. 116) attempted to explain the presence of waters of a similar chemistry (type Z) throughout the transition from apparent overpressure to underpressure (fig. 9), first stating that "if the type Z water is meteoric in origin, it cannot be circulating now," and then concluding that "the abnormally high pressure in the Morrow sand and the presence of the dilute type Z water in that area indicate that they have been effectively isolated hydraulically. The relatively dilute waters, therefore, may not be of meteoric origin, but rather water somehow removed from the normal processes of concentration." In summary, both water chemistry and petrophysical properties reflected in the well logs indicate that the current pressure state of the Morrow Formation differs from an earlier condition.

# Indicators of Paleopressure from Reduction in Resistivity

Following the finding by Breeze (1970), we examined resistivity logs from the Anadarko deep basin and shelf in Oklahoma, Texas, and Kansas. Our collection of sonic logs was not adequate for interpreting indicators of paleopressure, but the resistivity logs provided enough coverage and consistency that a shale trendline could be determined.

## Procedure

Approximately 175 resistivity logs were inspected for indications of paleopressure. A resistivity trendline was established in each well based on the resistivity of mudrocks in strata below the evaporites and limestones of Permian age (figs. 11and 12). Mudrocks were identified by high gamma-ray and high neutron porosity readings, which were made distinguishable by shading the gamma-ray log where it exceeded 70 American Petroleum Institute (API) units and by shading the neutron log where it exceeded a neutron porosity of 20 percent—this rule of thumb was varied somewhat in wells where the gamma-ray or neutron log required shifting. The resulting trendline represents the normal resistivity compaction trend for that well. In many wells, the resistivity log follows the trendline without a reversal throughout the Pennsylvanian siliciclastic sequence, as in the example of the West Edmond well (fig. 11). The resistivity is less than the trendline in sandstones, as indicated by yellow shading in the resistivity curve, but not in the mudstones. Because no resistivity reversal is discernible in the West Edmond well, rocks in this area were either never overpressured or else the paleopressure signature was not retained. The density log also increases steadily with depth, also indicating a normal compaction trend.

In other wells, the resistivity trend in mudstones reverses and decreases with depth rather than continuing to increase along the trendline. The depth of the first clear separation between the resistivity log and the trendline is selected and recorded; this depth is considered to be the top of paleopressure. For example, in the Bredy well (fig. 12), the top of paleopressure is located at a depth of 9,000 ft. Resistivity then decreases further with depth below the top of paleopressure although the trendline indicates that resistivity would increase in the absence of the effect of paleopressure; the separation between the two is made visible by the red shading. Within the Springer Formation at 14,800 ft, resistivity in mudstones is around 2 ohm-m where the trendline value is greater than 10 ohm-m. The sonic slowness in mudrocks tends to be higher within the paleopressured zone rather than lower as it would be under a normal compaction gradient. For example, at depths of 7,000 and 8,400 ft, sonic slowness is around 80 (μs/ft), but in deeper zones where resistivity is less than the resistivity trendline, as at 12,300 and 14,300 ft, the sonic slowness is around 90 μs/ft.

After eliminating wells that were not suitable for our study because of incomplete well logs or insufficient depth of penetration, 175 wells were used in this study. Of these, 68 wells displayed no reversal in the resistivity log, that is, the resistivity of mudrocks increased steadily along the trendline determined for that well. Wells in which the resistivity reversal is absent establish the eastern, western, and northern limits of the area of paleopressure. The top of paleopressure was established in the remaining 107 wells and based on formation tops for each well, the approximate geologic age of the top of paleopressure was assigned in terms of Pennsylvanian provincial series (Morrowan, Atokan, Desmoinesian, Missourian, or Virgilian). Formation tops of Springer age were included within the Morrowan Series. Twenty-four wells in the northwestern part of the study area display reduced resistivity values in the Morrow Formation but not above or below the Morrow.

Selected resistivity logs are presented in map format on plate 2 to provide an overview of the resistivity variations throughout the Anadarko Basin. The geographic variation of resistivity and paleopressure indicators can also be examined on one west-east (pl. 3) and three south-north cross sections (pls. 4–6). The tops of one formation boundary and four provincial series boundaries are also shown on plates 3–6, along with a line labeled "top of paleopressure," that marks the shallowest depth where resistivity falls below the trendline value. The locations and elevations of the resistivity reversals for the 44 wells on the four cross sections in plates 3–6 are given in Appendix 1.

The top of the reversal in resistivity could be picked with a high level of certainty in some wells but with less certainty in other wells, depending on such factors as the thickness and abundance of mudrock units, the presence and quality of the neutron log, and the slope of the trendline. For example, of the 13 wells in Line *C*–*C*' (pl. 5), inspection shows that the top of

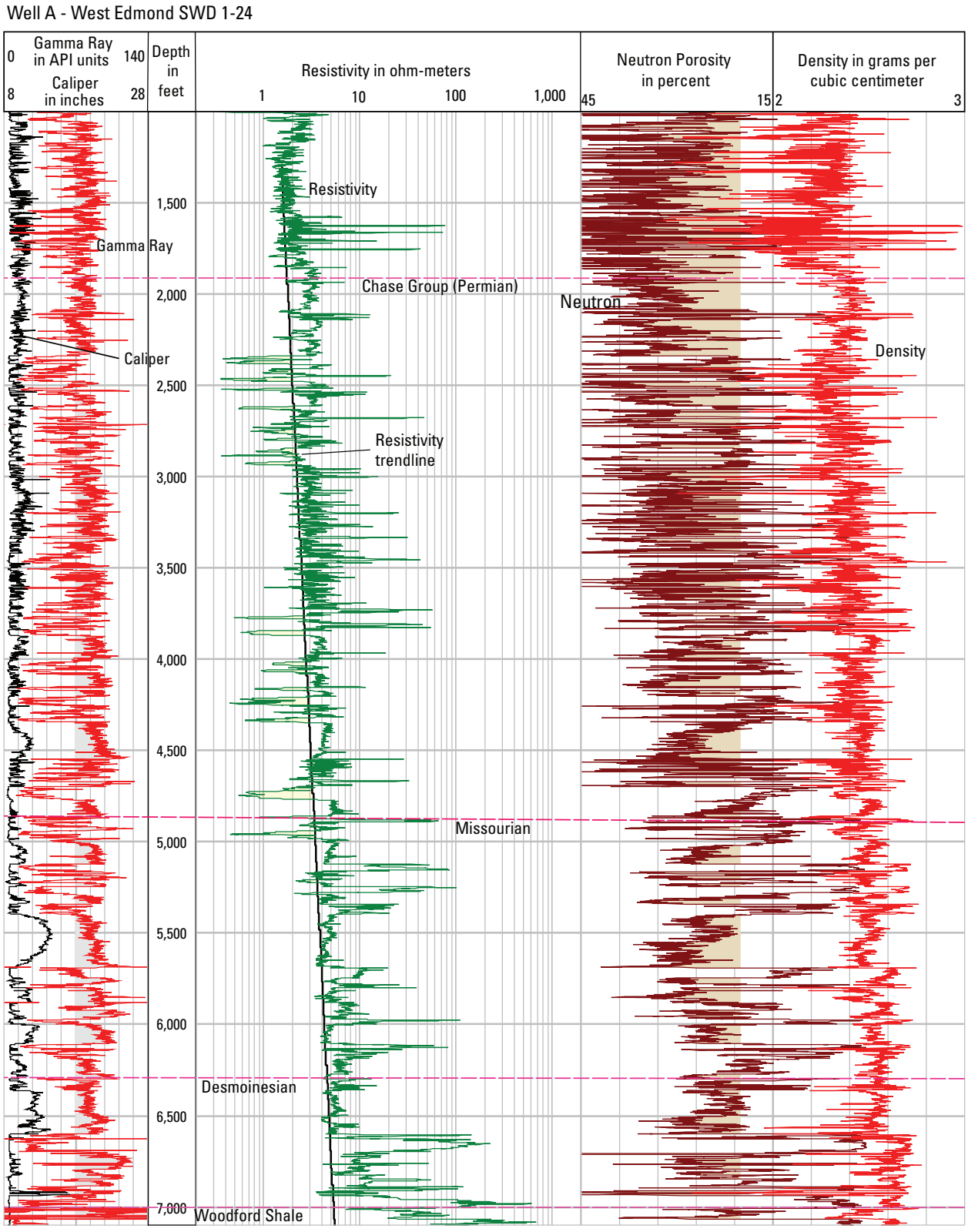


**Figure 11.** Gamma-ray, resistivity, neutron, and density logs in the West Edmond SWD 1-24 well (location shown on plate 2). Resistivity trendline is based on lowest resistivity values in mudrocks, which are represented by gamma-ray values in excess of 70 American Petroleum Institute (API) units (gray shading) and neutron porosity in excess of 20 percent (brown shading). Low resistivity in sandstones (light yellow shading) is attributed to saline water in the pore space. In this well, resistivity and density in mudrocks increase steadily with depth and there is no indication of paleopressure.

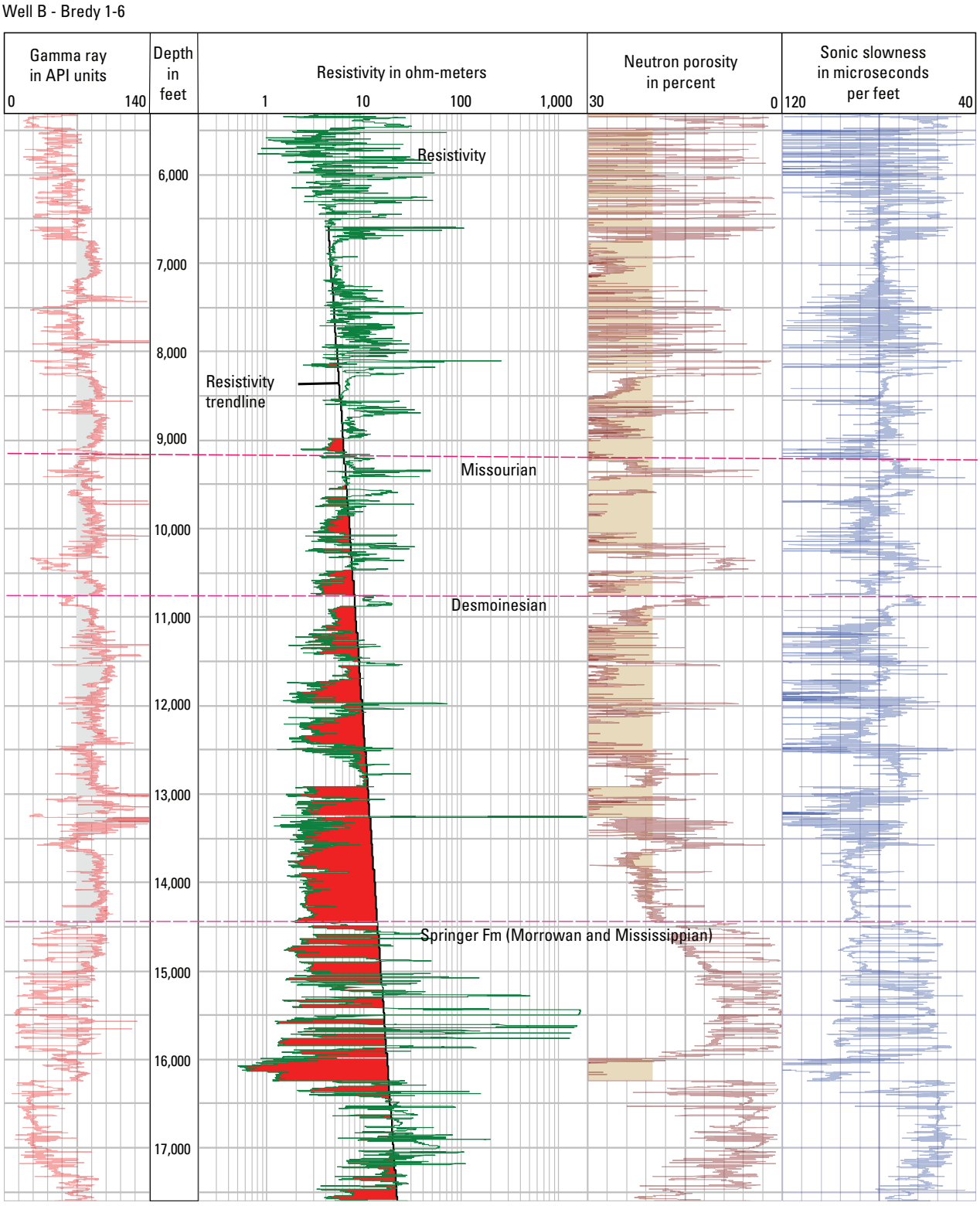


**Figure 12.** Gamma-ray, resistivity, neutron, and sonic logs in the Bredy well. The resistivity trendline is based on the lowest resistivity values in mudrocks above 9,000 feet, which are represented by gamma-ray values in excess of 70 American Petroleum Institute (API) units (gray shading) and neutron porosity in excess of 20 percent (brown shading). In this well, the top of paleopressure is at 9,000 feet. Below the top of paleopressure, resistivity in mudrocks decreases with increasing depth and sonic slowness in mudrocks increases with depth.

the reversal could not have been picked at a shallower depth in 6 wells, but could have been picked at a shallower depth in the other 7 wells, with a range of 147 to 710 ft. Similarly, the top of the reversal could not have been picked at a deeper depth in 5 wells but could have been picked at a deeper depth in the other 8 wells, with a range of 64 to 297 ft. Because the errors are not normally distributed, it is difficult to estimate an overall error, but it does appear that a typical error is several hundred feet in about half of the wells.

## Results

The geographic overview (pl. 2) shows how the paleopressure indicator varies with well position in the basin. The red shading between the trendline and the resistivity log indicates the presence of mudrocks, as determined by high gamma-ray (typically greater than 70 API units) or high neutron porosity (typically greater than 20 percent) readings. Resistivity is more reduced with respect to the trendline in the deeper part of the basin than on the flanks. Two maps show the elevation of the top of paleopressure (fig. 13) and the age of formations of the top of paleopressure (fig. 14).

The slope of the trendline is steepest on the flanks of the basin and not as steep in the deep basin, that is, resistivity increases with depth at a greater rate in the deep basin than on the flanks of the basin (pl. 2). This is not unexpected, as compaction determines the increase of resistivity with depth and compaction is greatest where burial depths are greatest. As a consequence, the width of the separation between the resistivity curve and the trendline is greatest in the deep basin, so the red shading is more obvious (fig. 12). Wells in which the shale resistivity decreases to less than 1/10 of the trendline value are outlined with a red circle in figure 13; these wells are mostly in the southeastern part of the Anadarko Basin.

The zone of paleopressure is bounded on the west and east by wells with no resistivity reversal, indicating no evidence of paleopressure (see plate 2 and wells on the west and east end of line *A–A′* in plate 3). All strata are thinner on the shelf than in the deep basin, and as strata thin the zone of paleopressure also thins becoming more difficult to discern, as shown in the northern most wells on lines *B–B′*, *C–C′*, and *D–D′* (pls. 4-6). At the northern edge of the area, the paleopressure indicators reduce in number and thickness, until it is not possible to determine whether paleopressure is present or not. For this reason, no effort was made to trace the extent of paleopressure into southern Kansas, with the exception of the wells in the southwestern counties. In southwestern Kansas, paleopressure is only visible in strata of Morrowan age (pl. 2) with the exception of a single well in which the top of paleopressure is in Desmoinesian age rocks (fig. 14).

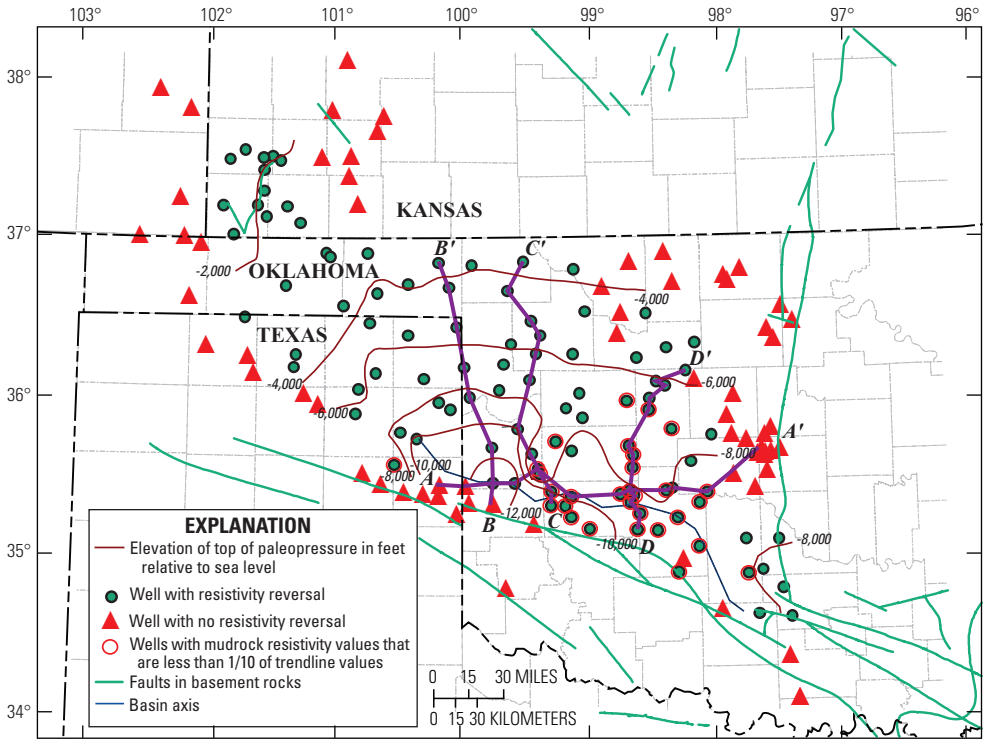


**Figure 13.** Map of the elevation of top of paleopressure as determined from resistivity logs. Lines *A–A′* through *D–D′* show location of cross sections on plates 3–6. A resistivity reversal was found in 107 wells (green circles) but was absent in 68 wells (red triangles).

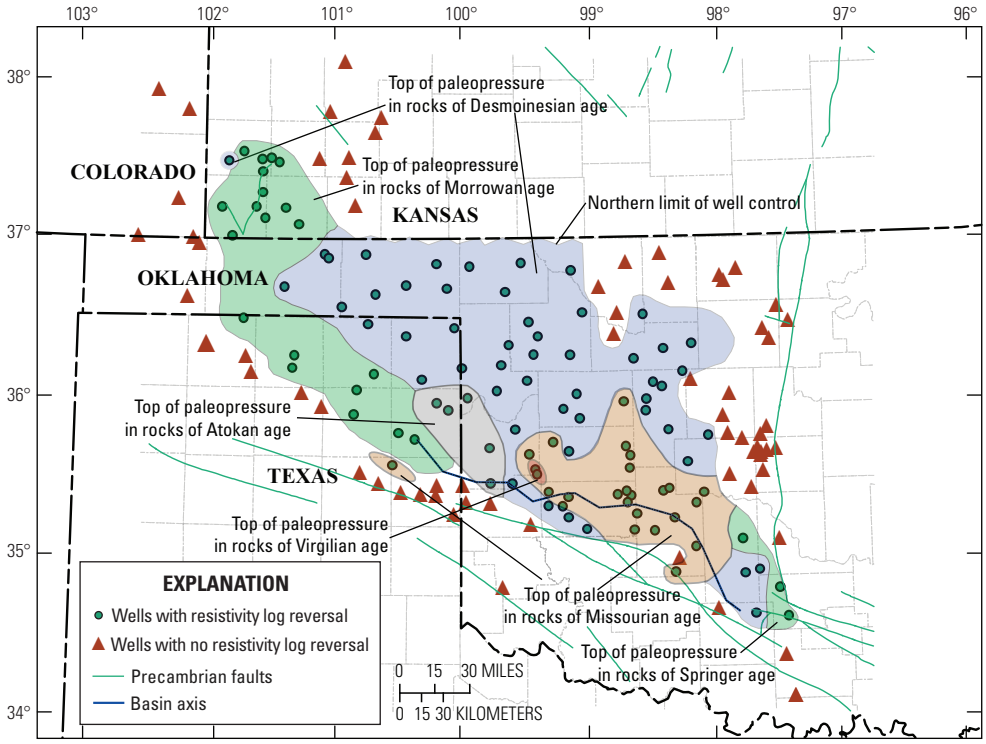


**Figure 14.** Map of age of rock unit containing top of paleopressure, based on the depth where the resistivity log changes from increasing downwards to decreasing downwards. The green area includes rocks of either Morrowan or Springer age, or both.

The changing relation between the top of paleopressure and rock unit age from west to east is seen by comparing the three north-south sections in plates 4–6. On the westernmost line *B–B′* (pl. 4), the top of paleopressure lies within the lower Desmoinesian or Atokan, within 500 ft above the informal Thirteen Finger lime, which is considered to be a source rock (Higley, chapter 7 of this report). The same relation holds over the northern portion of line *C–C′* (pl. 5), but in the southern part of line *C–C′*, paleopressure extends stratigraphically upwards into rocks of early Virgilian age in wells Bobby 1-14 and Weatherly 1. The upward extension of paleopressure produces a large southward deflection of the 8,000-ft contour in figure 13, encompassing a lobate area of approximately 15 by 30 miles where the top of paleopressure is higher in elevation (fig. 13) and higher stratigraphically (fig. 14) than immediately to the west and east. On the easternmost of the three south-north cross sections, the top of paleopressure lies within rocks of Missourian age in the eight wells on the southern part of the line (pl. 6, fig. 14). The elevation of the top of paleopressure is fairly constant over a distance of about 50 miles, as can be seen in plate 6 and by the wide separation between the 6,000- and 8,000-ft contours of figure 13. Line *A–A′* (pl. 3) also shows the general west to east stratigraphic climb of the top of paleopressure, interrupted by the high point into rocks of Virgilian age that is reached in the Weatherly well where line *A–A′* intersects line *C–C′*.

The top of paleopressure lies in rocks of Morrowan age along the west and northwest sides of the mapped area (fig. 14), with the exception of one outlying well in southwestern Kansas in which the paleopressure indicator extends into rocks of Desmoinesian age. The northwest-trending boundary between Morrowan and Desmoinesian age rocks is a transitional one because in some wells the resistivity reversals are in only a few thin units above the Thirteen Finger lime and cannot be unambiguously assigned to either Morrowan or Desmoinesian (Atokan units are absent or poorly defined in this area). The top of paleopressure does extend into recognizable Atokan units in five wells in an area straddling the Texas-Oklahoma border (fig. 14). Three wells in the southeastern edge of the basin show a clear indication of paleopressure in Springer mudrocks. Because there are no rocks older than Morrowan-Springer that show indications of paleopressure, areas marked Morrowan/Springer in figure 14 do not show evidence of paleopressure in any other sequences. Paleopressure extends stratigraphically upward from Desmoinesian rocks into Missourian rocks in the southeastern part of the study area and also in a single isolated well in the Texas Panhandle. As previously mentioned, the top of paleopressure extends into rocks of Virgilian age in two wells, as shown in fig. 14.

As can be seen in plates 2–6, the greatest depth extent of the paleopressure indicator lies in the deep basin; that is, the depth range from top of paleopressure to either the base

of paleopressure or the bottom of the well is greatest in the deep basin. Paleopressure extends downward through rocks of Morrowan age and into mudrocks of Mississippian age. Paleopressure does not register in Mississippian carbonates where mudrocks are absent. Somewhat surprisingly, the paleopressure indicator does not show up in the Devonian Woodford Shale (for example, Shirley 1-20 and Laubhan 35-1 wells of line *B–B′*, pl. 4; Vierson and Coram A1 wells of line *C–C′*, pl. 5). However, the Ordovician Sylvan Shale does produce a reduction in resistivity that shows up as a paleopressure indicator (Schneider 1 well, line *C–C′*, pl. 5; Girard 1 well, line *A–A′*, pl. 3).

## Comparison of Overpressured and Paleopressured Areas

The area of paleopressure is much more extensive than that of present-day overpressure. The contraction of both areal and vertical extents are shown in figures 15–17. In these figures, the outlines of paleopressure are derived from figure 14, accounting for the fact that areas of paleopressure are stacked such that paleopressure exists in Morrowan (the oldest) through Virgilian (the youngest) rocks in the small area where the top of paleopressure extends to rocks of Virgilian age, paleopressure exists in Morrowan through Missourian rocks in the brown-shaded area where the top of paleopressure extends upward into rocks of Missourian age, and so on. The outlines of overpressured areas in Desmoinesian and Morrowan rocks are taken from figures 6 and 7 and the outline of overpressured areas in Missourian rocks, not previously displayed, is shown in figure 14. Figures 15–17 show that (1) the outline of present-day overpressure at 0.5 psi/ft in rocks of Morrowan and Springer age is less than half of its respective area of paleopressure (fig. 15), (2) the area of present-day overpressure for Desmoinesian age rocks is less than half the area of paleopressure for Desmoinesian-age rocks (fig. 16), and (3) for Missourian age rocks, the outline of present-day overpressure is less than one-fourth that of the area of paleopressure (fig. 17). (Based on evidence from mud logs and gas flares, the area of present-day overpressure in Missourian age rocks is greater than shown in figure 17 [John Mitchell, oral commun., 2011)].) In all three cases, the area of present-day overpressure is substantially less than the area of paleopressure.

The vertical extents of paleopressure and overpressure are more difficult to compare than the horizontal extents. North of the overpressured area, defined by the 0.5 psi/ft contours (figs. 15–17), overpressure is not present but paleopressure has a finite vertical extent. Within the overpressured areas, the situation is mixed. Where paleopressure extends upward into younger rocks of Virgilian age, as shown in figure 14 and in the southward bowing of the -8,000-ft contour in figure 13, the top of paleopressure is clearly at a higher elevation than the top of overpressure. In other areas, the two surfaces appear to be at comparable elevations (compare fig. 13 with fig. 5), suggesting that there has been little downward movement of the overpressured zone. In a few areas, the top of paleopressure is at a lower elevation than the top of overpressure. These lower-elevation areas are where well coverage for paleopressure is sparse, so the counter-intuitive relation of a paleopressure surface deeper than an overpressure surface is discounted as an artifact of inadequate coverage. In summary, it appears that the top of the original overpressured volume has moved downward a few thousand feet in some locations, but overall there has been little downward movement of the top of the original overpressured volume.

A somewhat analogous setting exists in the Green River Basin of Wyoming, where Jonah field, a fault-bounded, overpressured tight gas system lies within an extensive area of normally pressured strata. Resistivity and sonic logs display trend reversals at the top of the overpressured gas system in Jonah Field. The reversals are also at the same stratigraphic level in wells in non-productive, normally pressured Tertiary strata outside the field, where the well log signatures and present-day pressure are decoupled (Cluff and Cluff, 2004). Cluff and Cluff (2004) concluded that the well log reversals record pressure conditions at the time of maximum burial, and that the "signature was frozen into the rocks during subsequent exhumation" making Jonah Field "an anomalous remnant" of a former regional overpressured area (Cluff and Cluff, 2004, p. 143).

Thermal maturity maps based on petroleum system modeling (chapter 3 of this report) provide contours of vitrinite reflectance ($R_o$) that can be compared with the outlines of paleopressure and present-day overpressure (figs. 15–17). In Morrowan age rocks, most of the overpressured area within the 0.7 psi/ft boundary lies within the 1.2% $R_o$ contour, and almost all of the 0.5 psi/ft area lies within the 0.8% $R_o$ contour (fig. 15). However, a substantial part of the paleopressured area lies outside the 0.8 percent contour. In Desmoinesian age rocks (fig. 16), the 1.2% $R_o$ contour roughly coincides with the 0.7 psi/ft contour, showing that the highest present-day overpressures are in the same area as the levels of thermal maturity associated with gas generation. The 0.8% $R_o$ contour includes most of the area within the 0.5 psi/ft contour but does not include all of the paleopressured area in rocks of Desmoinesian age. For comparison with paleopressured and present-day overpressured areas of Missourian age rocks (fig. 17), we display the contours of 0.8% $R_o$ and 1.0% $R_o$ from a model for the Douglas Group of early Virgilian age, which immediately overlies rocks of Missourian age. No $R_o$ values higher than 1.0 percent were computed for this model. The areas of paleopressure and present-day overpressure (fig. 17) coincide with part of the area circumscribed by a 0.8% $R_o$ contour.

In summary, the comparisons among overpressured areas, paleopressured areas, and $R_o$ contours from petroleum system modeling (figs. 15–17) show that (1) the areas of high overpressure and high $R_o$ values are comparable in Morrowan and Desmoinesian rocks, (2) most of the overpressured areas lie within the 0.8% $R_o$ contours, and (3) paleopressured areas generally extend beyond the 0.8% $R_o$ contours.

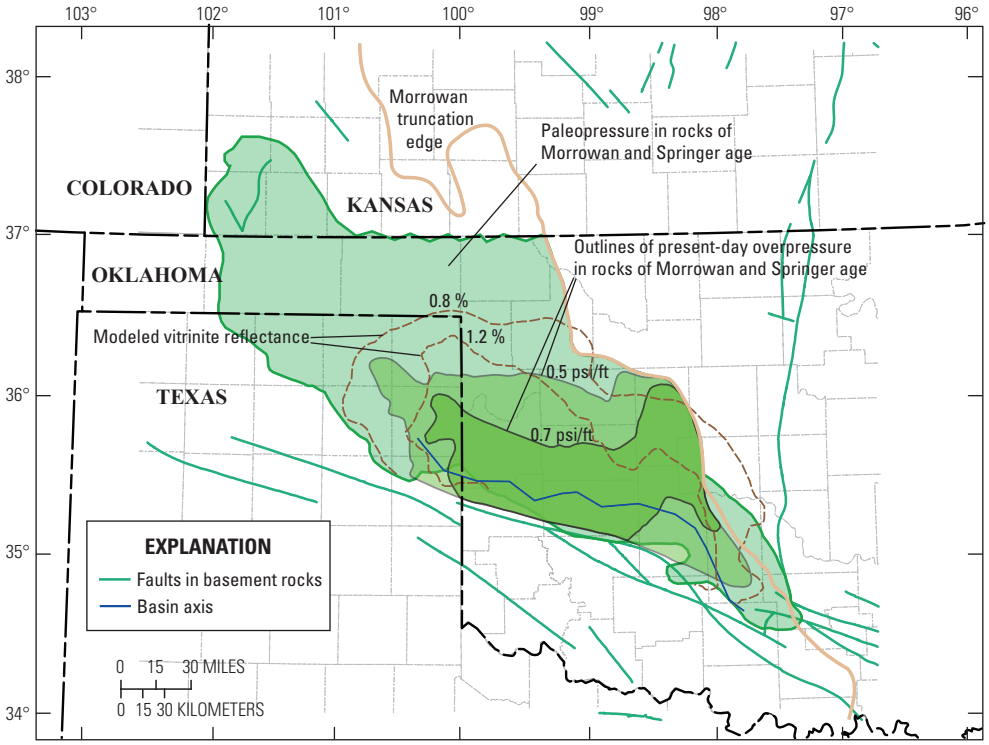


**Figure 15.** Map showing extents of paleopressure and overpressure in rocks of Morrowan and Springer age. The extent of the paleopressure indicator from resistivity logs is derived from figure 14 and the extent of present-day overpressure from pressure data is taken from figure 7. Modeled vitrinite reflectance contours of 0.8 and 1.2 percent for source rocks of Thirteen Finger lime of Atokan age taken from Higley (chapter 7 of this report).

The continued existence of an overpressured zone long after the cessation of burial and hydrocarbon generation has perplexed a number of investigators because containment of overpressure for long time periods requires extremely low values of permeability to fluid flow on the top, bottom, and sides of the overpressured volume. Using a one-dimensional model of pressure dissipation and parameters relevant to the Anadarko Basin, Lee and Deming (2002) observed that the retention of pressure from either compaction disequilibrium or hydrocarbon generation (with uplift) requires permeability in seals of 100-m thickness to be so low as to be effectively zero. In a related report, Deming and others (2002) discuss the dilemma of long-lived overpressured volumes in the Anadarko Basin (and in sedimentary basins in general) and contribute a possible explanation for the retention of fluids within the basins. The explanation relies on laboratory experiments reported by Shosa and Cathles (2001), in which water flowing through a layered sand pack with flow rates and pressures governed by Darcy's law ceased flowing when gas was introduced into the system. Experimental checks verified that the cessation of flow was caused by gas bubbles immobilized at the interfaces between coarse and fine sand packs. Deming and others (2002) extrapolated the laboratory work to the basin scale, using well logs to show that the requisite number of fine-grain/coarse-grain interfaces are present in the Anadarko Basin.

The question of timing of the contraction of the overpressured area from its original (paleopressured) extent to its present configuration is another difficult question, and depends upon the chosen explanation for the retention of overpressure. The presence of underpressure in the northern and western parts of the basin is documented in a companion report by Nelson and Gianoutsos (chapter 9 of this report) and the timing of its development is conjectured to be quite recent in geological time. Assuming that the mechanism reported by Shosa and Cathles (2001) was (and is still) operative, then it is plausible that as erosion exposed Permian and Pennsylvanian strata, the pressure gradients changed direction in such a way as to render the gas-bubble lockup no longer effective on the northern flank of the basin. Moreover, the conversion from an overpressured system to a normal/underpressured system may be ongoing at the northern edge of the present-day overpressured area.

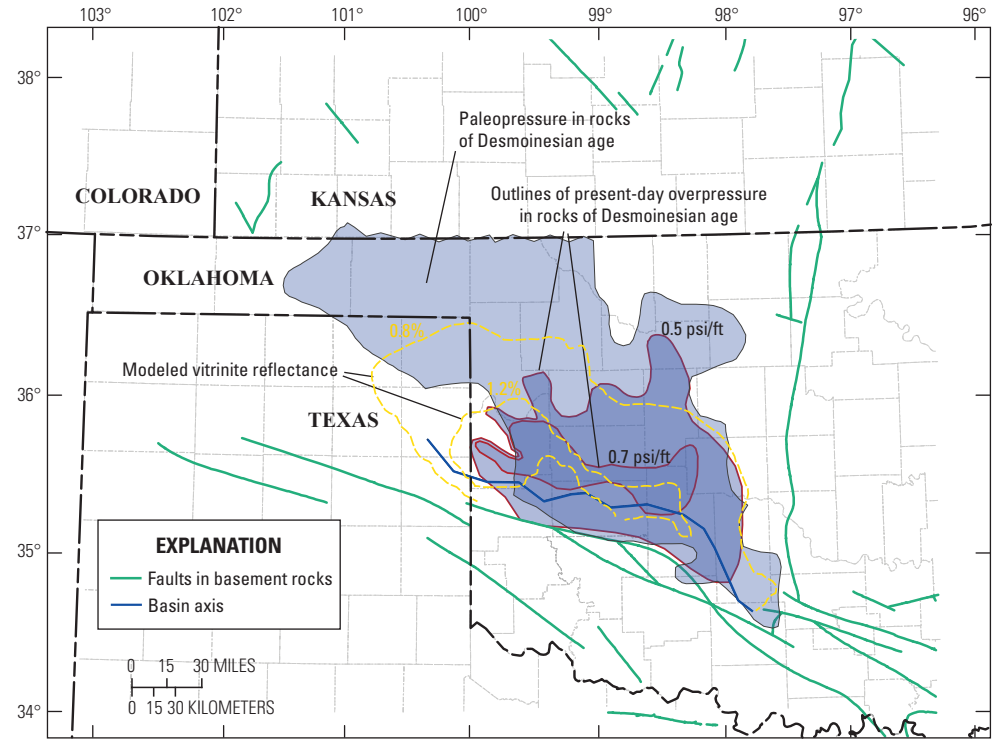


**Figure 16.** Map showing extents of paleopressure and overpressure in rocks of Desmoinesian age. The extent of the paleopressure indicator from resistivity logs is derived from figure 14 and the extent of present-day overpressure from pressure data is taken from figure 6. Modeled vitrinite reflectance contours of 0.8 and 1.2 percent for source rocks of Desmoinesian age taken from Higley (chapter 7 of this report).

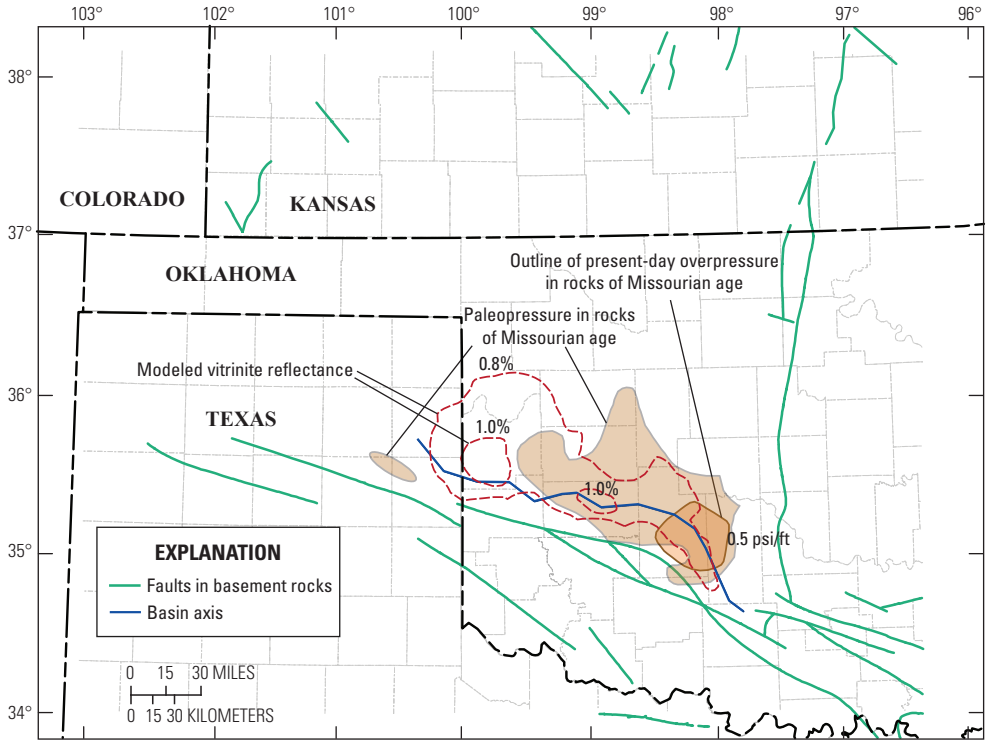


**Figure 17.** Map showing extents of paleopressure and overpressure in rocks of Missourian age. The extent of the paleopressure indicator from resistivity logs is derived from figure 14. Modeled vitrinite reflectance contours of 0.8 and 1.0 percent for source rocks of early Virgilian age taken from Higley (chapter 7 of this report).

## Summary and Conclusions

Our review of the state of overpressure in the Anadarko Basin shows (1) the prevalence of normal to subnormal pressures on the northern flank of the basin (pl. 1, fig. 4), (2) the progressive deepening of the top of overpressure from north to south (pl. 1, fig. 5), (3) the increasing vertical extent of overpressure from north to south as strata thicken (pl. 1), and (4) the distinct compartmentalization of overpressure in rocks of Desmoinesian and Morrowan age (pl. 1).

The area of overpressure in rocks of Desmoinesian age is roughly 100 miles in the west-northwest direction and 50 miles in the east-northeast direction, based on the 0.5 psi/ft contour (fig. 6). The area of highest pressures within the 0.7 psi/ft contour nearly coincides with the 1.2% $R_o$ contour (fig. 16), illustrating a close connection between high present-day overpressure and a thermal maturity level that is considered to be the end of oil generation for the Devonian-Mississippian Woodford Shale (chapter 3 of this report). The area of overpressure in rocks of Morrowan age is greater than 150 miles in the west-northwest direction and greater than 50 miles in the east-northeast direction, based on the 0.5 psi/ft contour (fig. 6). The area of highest pressures within the 0.7 psi/ft contour lies mostly within the 1.2% $R_o$ contour (fig. 15). Evaluation of a dataset from Powley (1984) strengthens the case for subcompartments within strata of Morrowan age and establishes the existence of pressure gradients of 0.465 psi/ft at elevated overall pressures in three of the subcompartments (fig. 8). These gradients show that water, not gas, is the continuous fluid within the subcompartments.

Reversals in resistivity logs from a normal mudrock compaction trend are most manifest in the deep basin and persist northward onto the shelf, but do not exist in wells east and west of the basin (pls. 2–5 and figs. 13–14). The top of the trend reversals lies in Virgilian and Missourian rocks in the deep basin and in Morrowan rocks on the western and southeastern fringes of the system (fig. 14), although the pattern with regard to rock age is an irregular one. The resistivity trend reversals in Desmoinesian rocks extend to the Oklahoma-Kansas border and may have extended farther to the north, but the top of the trend reversal cannot be selected with confidence where strata thin on the northern flank of the basin.

Equating the resistivity trend reversals with paleopressure allows comparisons between the areal and vertical extents of the paleopressured system with the extents of the present-day overpressured system. The areal extents of paleopressure are substantially larger, about twice as large, as the areal extents of present-day overpressure in rocks of Morrowan, Desmoinesian, and Missourian age (figs. 15–17). Changes in vertical extent, however, are more subtle and more difficult to determine. Although the high points of the original overpressured volume have moved downwards a few thousand feet in some locations, overall there has been little downward migration of the top of the original overpressured volume. The largest reductions in resistivity relative to trendlines, and correspondingly the most profound expressions of paleopressure, are in an area that extends for 100 miles in a northwesterly direction more or less aligned with the basin axis and extending 20 to 40 miles north from the basin axis (pls. 3–6, fig. 13). This area of large reductions in resistivity coincides with the area where paleopressures extended into rocks of Missourian age (fig 14).

The contraction of the paleopressured area to the area of present-day overpressure could conceivably have occurred over any span of geological time since the end of Permian deposition. However, it seems likely that the contraction occurred when the pressure reference for strata on the northern flank of the basin was established as erosional processes exposed strata of Permian and Pennsylvanian age at the eastern edge of the basin.

## Acknowledgments

James Puckette, of the Geology Department at Oklahoma State University, provided access to files of pressure data from the publication by Al-Shaieb and others (1994a). Elena Hickman, U.S. Geological Survey (USGS) contractor, provided registered digital maps. Debra Higley, USGS, provided formation tops and other geological information. Many constructive review comments by Noel Osborne, USGS, led to revisions that have improved the clarity of the chapter of the report.

## References Cited

Al-Shaieb, Z., Puckett, J.O., Abdalla, A.A., and Ely, P.B., 1994a, Megacompartment complex in the Anadarko Basin: A completely sealed overpressured phenomenon, *in* Ortoleva, Peter J., ed., Basin compartments and seals: American Association of Petroleum Geologists Memoir 61, p. 55–68.

Al-Shaieb, Z., Puckett, J.O., Abdalla, A.A., and Ely, P.B., 1994b, Three levels of compartmentation within the overpressured interval of the Anadarko Basin, *in* Ortoleva, Peter J., ed., Basin compartments and seals: American Association of Petroleum Geologists Memoir 61, p. 69–83.

Bigelow, E.L., 1994, Well logging methods to detect abnormal pressure, *in* Fertl, W.H., Chapman, R.E., and Hotz, R.F., eds., chap. 7, Studies in abnormal pressure: Developments in Petroleum Science 38, Amsterdam, Elsevier, 454 p.

Breeze, A.F., 1970, Abnormal-subnormal pressure relationships in the Morrow sands of northwestern Oklahoma: University of Oklahoma, M.S. thesis, 122 p.

Carter, L.S., Kelley, S.A., Blackwell, D.D., and Naeser, N.D., 1998, Heat flow and thermal history of the Anadarko Basin, Oklahoma: American Association of Petroleum Geologists Bulletin, v. 82, no. 2, p. 291–316.

Cluff, R.M., and Cluff, S.G., 2004, The origin of Jonah Field, northern Green River Basin, Wyoming, chap. 8 *in* Robinson, J.W., and Shanley, K.W., eds.: Jonah Field: Case study of a tight-gas fluvial reservoir: AAPG Studies in Geology 52 and Rocky Mountain Association of Geologists 2004 Guidebook, p. 127–145.

Deming, D., Cranganu, C., and Lee, Y., 2002, Self-sealing in sedimentary basins: Journal of Geophysical Research, v. 107, n. B12, 2329, 9 p.

Dickey, P.A., and Soto, C., 1974, Chemical composition of deep subsurface waters on the western Anadarko Basin: Society of Petroleum Engineers Paper 5178, 17 p.

IHS Energy, 2009, U.S. production and well data: database available from IHS Energy, 15 Inverness Way East, D205, Englewood, CO 80112.

Lee, Y., and Deming, D., 2002, Overpressures in the Anadarko Basin, southwestern Oklahoma: Static or dynamic?: American Association of Petroleum Geologists Bulletin, v. 86, n. 1, p. 145–160.

Powley, D.E., 1984, Subsurface fluid compartments: American Association of Petroleum Geologists Search and Discovery Article 60006 (2006), adapted from Amoco Geological Research Report, 52 p. accessed December 14, 2010, at *http://www.searchanddiscovery.com/documents/2006/06015powley/images/powley01.pdf*.

Shosa, J.D. and Cathles, L.M., 2001, Experimental investigation of capillary blockage of two phase flow in layered porous media, *in* Fillon, R.H. and others eds., Petroleum systems of deep-water basins: Global and Gulf of Mexico experience: 21st Annual Bob F. Perkins Research Conference [CD-ROM], Gulf Coast Section, Society of Economic Paleontological and Mineralogical Society, Houston, Texas.

U.S. Geological Survey, 2014, Colorado, Kansas, New Mexico, Oklahoma, and Texas: U.S. Geological Survey digital data, The National Map, accessed August 4, 2014, at: *http://viewer.nationalmap.gov/viewer/*.

# Appendix 1

List of wells shown on cross sections on plates 3–6 (Excel file format).

| API number | Lease name | No. | Operator | State | County | Reference elevation, in feet | Reference | Latitude | Longitude | Section | Township | Range | Rock unit at top of resistivity reversal | Depth of top of resistivity reversal, in feet | Elevation of top of resistivity reversal, in feet | Cross section |
|---|---|---|---|---|---|---|---|---|---|---|---|---|---|---|---|---|
| 3501723998 | West Edmond Swd | 1-24 | Chesapeake Operating Inc | Oklahoma | Canadian | 1,159 | DF | 35.669 | -97.683 | 24 | 14N | 05W | Absent | -- | -- | A |
| 4248330610 | Miles Gas Unit | 1 | Exxon Corporation | Texas | Wheeler | 2,509 | KB | -- | -- | RRC Dist 10, Sec 2 | Blk A-4 | Survey: H&GN | Absent | -- | -- | A |
| 4248331989 | Hagermann 21 | 1 | Chesapeake Operating Inc | Texas | Wheeler | 2,164 | KB | 35.433 | -100.00 | RRC Dist 10, Sec 21 | BLK OS2 | Peter-man CE Survey | Absent | -- | -- | A |
| 3512920675 | Millington-Shields | 1 | El Paso Natural Gas Company | Oklahoma | Roger Mills | 2,158 | GR | 35.454 | -99.589 | 1 | 11N | 23W IM | Desmoinesian | 14,600 | -12,409 | A |
| 3501520950 | Tillman | 1 | Monsanto Company | Oklahoma | Caddo | 1,475 | DF | 35.418 | -98.355 | 22 | 11N | 11W IM | Missourian | 9,485 | -8,008 | A |
| 3501522365 | Lindley | 3-30 | Apache Corporation | Oklahoma | Caddo | 1,427 | GR | 35.402 | -98.401 | 30 | 11N | 11W IM | Missourian | 9,090 | -7,639 | A |
| 3501721307 | Girard | 1 | Key Operating Company | Oklahoma | Canadian | 1,455 | DF | 35.388 | -98.083 | 31 | 11N | 08W IM | Missourian | 9,550 | -8,094 | A |
| 3514920050 | Richert | 1 | Conoco Inc | Oklahoma | Washita | 1,607 | KB | 35.382 | -98.760 | 35 | 11N | 15W IM | Missourian | 9,665 | -8,058 | A |
| 3514920342 | Hohnke Leo Unit | 1 | Exxon Corporation | Oklahoma | Washita | 1,849 | DF | 35.367 | -99.149 | 6 | 10N | 18W IM | Missourian | 11,600 | -9,750 | A |
| 3501721288 | Royse | 1 | Samedan Oil Corporation | Oklahoma | Canadian | 1,342 | GR | 35.504 | -97.906 | 23 | 12N | 7W IM | Absent | -- | -- | A |
| 3512920639 | A H Douglas Estate | 1 | Exxon Corporation | Oklahoma | Roger Mills | 2,277 | DF | 35.456 | -99.759 | 5 | 11N | 24W | Atokan | 17,000 | -14,753 | A, B |
| 3512930019 | Weatherly | 1 | Petroleum Waste Recovery Inc | Oklahoma | Roger Mills | -- | -- | 35.543 | -99.406 | 3 | 12N | 21W IM | Virgilian | 8,730 | -6,678 | A, C |
| 3514920232 | Davis | 28-1 | Getty Oil Company | Oklahoma | Washita | 1,601 | DF | 35.403 | -98.689 | 28 | 11N | 14W IM | Missourian | 9,200 | -7,598 | A, D |
| 3500921156 | Cat Creek | 1-19 | Chesapeake Operating Inc | Oklahoma | Beckham | 2,045 | DF | 35.329 | -99.786 | 19 | 10N | 24W | Absent | -- | -- | B |
| 3504520748 | Laubhan 35 | 1 | Marathon Oil Company | Oklahoma | Ellis | 2,370 | DF | 35.996 | -99.940 | 35 | 18N | 26W | Atokan | 11,090 | -8,705 | B |
| 3500720640 | Dixon | 1-6 | King Resources Company | Oklahoma | Beaver | 2,491 | DF | 36.839 | -100.188 | 6 | 04N | 27E CM | Desmoinesian | 6,300 | -3,807 | B |
| 3500721928 | Homes Or Holmes? | 36-2 | Home Petroleum Corporation | Oklahoma | Beaver | -- | -- | 36.684 | -100.105 | 36 | 03N | 27E CM | Desmoinesian | 6,745 | -4,368 | B |
| 3504521097 | Schoenhals | 1 | Marathon Oil Company | Oklahoma | Ellis | 2,450 | DF | 36.183 | -99.984 | 28 | 20N | 26W IM | Desmoinesian | 9,450 | -7,000 | B |
| 3512922603 | Shirley | 1-20 | The Ghk Company | Oklahoma | Roger Mills | 2,056 | DF | 35.679 | -99.768 | 20 | 14N | 24W | Desmoinesian | 13,580 | -11,524 | B |
| 4229531218 | Gadberry | 1-174 | Williford Energy Co | Texas | Lipscomb | 2,488 | KB | -- | -- | RRC Dist 10, Sec 174 | Blk 10 | Survey: H&GN | DesMonesian | 7,810 | -5,322 | B |
| 3512922522 | Bobby | 1-14 | Chesapeake Operating Inc | Oklahoma | Roger Mills | 2,007 | GR | 35.512 | -99.391 | 14 | 12N | 21W IM | Virgilian | 8,790 | -6,763 | C |
| 3504520879 | Coram A | 1 | Cities Service Company | Oklahoma | Ellis | 2,268 | DF | 36.103 | -99.468 | 20 | 19N | 21W IM | Desmoinesian | 9,580 | -7,293 | C |
| 3505921196 | Blasdel | 2 | Terra Resources Inc | Oklahoma | Harper | 1,759 | DF | 36.847 | -99.514 | 1 | 27N | 22W IM | Desmoinesian | 5,505 | -3,743 | C |
| 3505922317 | Horton | 1-11 | Chesapeake Operating Inc | Oklahoma | Harper | 2,125 | DF | 36.664 | -99.640 | 11 | 25N | 23W IM | Desmoinesian | 6,535 | -4,409 | C |
| 3512920125 | Viersen Unit | 1 | Pride Energy Company | Oklahoma | Roger Mills | -- | -- | 35.794 | -99.564 | 8 | 15N | 22W IM | Desmoinesian | 12,255 | -10,095 | C |
| 3515320043 | Everett Johns | 1-18 | A. R. Dillard Inc | Oklahoma | Woodward | 2,077 | GR | 36.383 | 99.379 | 18 | 22N | 20W | Desmoinesian | 7,405 | -5,316 | C |
| 3515321951 | Schneider | 1 | Plains Petroleum Operating Co | Oklahoma | Woodward | 1,896 | GR | 36.476 | -99.455 | 16 | 23N | 21W IM | Desmoinesian | 7,025 | -5,111 | C |

| API number | Lease name | No. | Operator | State | County | Reference elevation, in feet | Reference | Latitude | Longitude | Section | Township | Range | Rock unit at top of resistivity reversal | Depth of top of resistivity reversal, in feet | Elevation of top of resistivity reversal, in feet | Cross section |
|---|---|---|---|---|---|---|---|---|---|---|---|---|---|---|---|---|
| 3515322725 | Grunewald | 1-26A | Chesapeake Operating Inc | Oklahoma | Woodward | 2,165 | DF | 36.270 | -99.417 | 26 | 21N | 21W IM | Desmoinesian | 8,260 | -6,093 | C |
| 3514920705 | Niece | 3-27 | Meridian Oil Inc | Oklahoma | Washita | 1,828 | GR | 35.312 | -99.306 | 27 | 10N | 20W IM | DesMonesian | 11,400 | -9,535 | C |
| 3512923149 | Switzer | 4-32 | Apache Corporation | Oklahoma | Roger Mills | 1,755 | DF | 35.640 | -99.453 | 32 | 14N | 21W IM | Missourian | 9,150 | -7,395 | C |
| 3514920152 | Kilhoffer | 1-27 | The Ghk Company | Oklahoma | Washita | 2,019 | DF | 35.400 | -99.303 | 27 | 11N | 20W IM | Missourian | 12,100 | -10,079 | C |
| 3514920020 | Bertha Rogers | 1 | Lone Star Producing Company | Oklahoma | Washita | 1,922 | DF | 35.309 | -99.193 | 27 | 10N | 19W IM | Desmoinesian | 13,100 | -11,178 | C |
| 3501121816 | Wisdom | 1-5 | Sabine Production Company | Oklahoma | Blaine | 1,311 | DF | 36.062 | -98.401 | 5 | 18N | 11W IM | Desmoinesian | 7,540 | -6,227 | D |
| 3501122895 | Gypsum U S | 1-27 | Chesapeake Operating Inc | Oklahoma | Blaine | 1,595 | DF | 36.090 | -98.470 | 27 | 19N | 12W IM | Desmoinesian | 7,670 | -6,073 | D |
| 3501122962 | Chain | 1-6 | Chesapeake Operating Inc | Oklahoma | Blaine | 1,574 | DF | 35.982 | -98.525 | 6 | 17N | 12W IM | Desmoinesian | 8,250 | -6,676 | D |
| 3501123150 | Christensen | 1-36 | Chesapeake Operating Inc | Oklahoma | Blaine | 1,598 | DF | 35.910 | -98.532 | 36 | 17N | 13W IM | Desmoinesian | 8,580 | -6,980 | D |
| 3501123174 | Gwyn | 1-2 | Chesapeake Operating Inc | Oklahoma | Blaine | 1,166 | DF | 36.154 | -98.235 | 2 | 19N | 10W IM | Desmoinesian | 6,960 | -5,794 | D |
| 3501520860 | Allred | 18-1 | L G Williams Oil Company | Oklahoma | Caddo | 1,462 | GR | 35.258 | -98.611 | 18 | 9N | 13W IM | Missourian | 9,800 | -8,313 | D |
| 3503920435 | Swosu | 1 | Amoco Production Company | Oklahoma | Custer | 1,610 | DF | 35.548 | 98.661 | 3 | 12N | 14W IM | Missourian | 9,460 | -7,848 | D |
| 3503921952 | Wingard | 1-16 | Chesapeake Operating Inc | Oklahoma | Custer | 1,746 | DF | 35.685 | -98.689 | 16 | 14N | 14W IM | Missourian | 9,200 | -7,453 | D |
| 3503922053 | Pitzer | 1-2 | Zinke & Trumbo Inc | Oklahoma | Custer | 1,699 | DF | 35.628 | -98.655 | 2 | 13N | 14W IM | Missourian | 9,360 | -7,659 | D |
| 3514920141 | Seger Indian School | 1-21 | Hamilton Brothers Oil Company | Oklahoma | Washita | 1,601 | DF | 35.331 | -98.680 | 21 | 10N | 14W IM | Missourian | 9,610 | -8,004 | D |
| 3514920153 | Aaron Unit | 1 | Amoco Production Company | Oklahoma | Washita | 1,558 | DF | 35.374 | -98.653 | 2 | 10N | 14W IM | Missourian | 9,440 | -7,879 | D |
| 3514920202 | Arthur | 24-1 | Towner Petroleum Company | Oklahoma | Washita | 1,429 | DF | 35.156 | -98.633 | 24 | 8N | 14W IM | Missourian | 10,390 | -8,940 | D |

Explanation: IM, Indian Meridian; CM, Cimarron Meridian

Well names and locations from Oklahoma Corporation Commission (*www.occeweb.com*) and Railroad of Texas (*http://www.rrc.state.tx.us/*)